Evolution of salt structures of the Pyrenean rift (Chaînons Béarnais, France): From hyper-extension to tectonic inversion

Pierre Labaume, Antonio Teixell

Evolution of salt structures of the Pyrenean rift (Chaînons Béarnais, France): From hyper-extension to tectonic inversion

Pierre Labaume[a,*], Antonio Teixell[b]

[a]*Géosciences Montpellier, Université de Montpellier, CNRS, Université des Antilles, Montpellier, France (pierre.labaume@gm.univ-montp2.fr)*

[b]*Dpt. de Geologia, Universitat Autònoma de Barcelona, Bellaterra, Spain (antonio.teixell@uab.es)*

**Corresponding author*

ABSTRACT

The Chaînons Béarnais is a salt-detached fold belt in the northern Pyrenees that formerly occupied the axis of the Cretaceous Pyrenean rift. Geological map revision and cross-section construction from surface geology and industrial well and seismic reflection data emphasize the role of salt diapirism in the folding of the belt during the Cretaceous extension and the subsequent Pyrenean orogeny. Pre-rift Triassic evaporites played a fundamental role during rifting, allowing the sedimentary basin lying above to detach and slide down the hyper-extended margins onto a central exhumed mantle tract. Since the Early Cretaceous (and locally probably since the Jurassic) a system of low-amplitude salt walls evolved in shallow marine environments punctuated by episodic emersion. During the main stage of crustal extension, in late Aptian to early Cenomanian times, carbonate shelves rapidly drowned giving rise to deeper marine sedimentation. This was a period of major rise of salt walls, progressively detached from their substratum. These salt walls enclosed minibasins that accumulated thick flysch deposits arranged in growth stratal patterns. Depocenter migration and foundering of previous diapiric highs controlled further flysch deposition during the Late Cretaceous, while moderate extension probably persited until the onset of the Pyrenean compression. During the late Santonian to Paleogene Pyrenean orogeny, the sedimentary lid of the Chaînons Béarnais basin climbed back along the Triassic detachment onto the colliding continental margins, leading to salt wall squeezing and further rising. Based on the Cretaceous timing and style of growth folding, we suggest that salt wall squeezing was not solely related to the Pyrenean compression, but shortening affected the diapiric ridges during the syn-rift sliding by gravity and crowding in the basin center, as the rifted margins were pulled apart from beneath. This makes the Chaînons Béarnais belt a unique field analog for contractional salt-tectonic systems in distal continental margins.

Key words:
Salt tectonics
Minibasin
Continental margin
Hyper-extension
Tectonic inversion
Pyrenees

1. Introduction

Rifted continental margins with salt diapirism and large-scale gravitational sliding above salt units are commonly reported in modern settings (e.g. Rowan et al., 2004; Brun and Fort, 2011; Jackson and Hudec, 2017). Abundant seismic surveys have revealed the essential structural features on the salt-dominated margins, with both extensional and contractional structures above common salt detachments. However, these slid structures are located in distal offshore domains of modern margins, and salt detachment systems of ancient continental margins observable in outcrop after tectonic inversion are rarely reported. Recent works in the former peri-Iberian margins give valuable evidence of salt detachment associated to crustal hyper-extension and mantle exhumation in ancient, mid-Cretaceous rifts, containing salt-related extensional structures inverted during the Upper Cretaceous-Tertiary. Such features are now exposed in the northern Pyrenean belt (Jammes et al., 2009, 2010; Lagabrielle et al., 2010; 2019a and b, 2020; Teixell et al., 2016, 2018), the Basco-Cantabrian belt (Pedrera et al., 2017; Ducoux et al., 2019), or imaged by subsurface data in the offshore Parentis (Jammes et al., 2010; Ferrer et al., 2012) and Columbrets (Etheve et al., 2018) basins. A particular aspect of these peri-Iberian detachments is that they are located in the Middle-Upper Triassic evaporite facies, i.e. a salt-bearing layer which can be considered as pre-rift with respect to the main, Cretaceous-age extension. Hence, the salt-related structures potentially recorded the whole rift and post-rift history, in contrast with those modern margins where detachment occurred on post-rift salt (see references above) and is thus largely independent on the extensional structures in the underlying crust. In the Pyrenean mountain belt, the Triassic evaporite layer is commonly present in the fold and thrust belts of both the North and South-Pyrenean Zones (Fig. 1). This layer is well known to have acted as the main décollement layer for the orogenic thrust sheets (Séguret, 1972), and for the Mesozoic extensional structures (Jammes et al. 2009, 2010; Lagabrielle et al., 2010, 2019a and b, 2020; Teixell et al., 2016, 2018). It also promoted diapirism both during the rifting (Canérot, 1988, 1989; James and Canérot, 1999; Canérot et al., 2005; López-Mir et al., 2014; Saura et al., 2016; García-Senz et al., 2019) and the Pyrenean compression (Muñoz et al., 2013; Santolaria et al., 2014). However, the detailed interactions between the salt detachment and diapirism remain little discussed with the exception of Jammes et al. (2010).

In this paper, we describe diapiric structures originated in the Cretaceous margins of the west-central Pyrenean rift and inverted by the Pyrenean orogeny in the so-called Chaînons Béarnais belt (Fig. 2). Moderate contractional inversion uplifted and exhumed the extensional system without destroying its major features. The diapiric origin of the Chaînons Béarnais folds and thrusts is put forward in previous works (Canérot, 1988, 1989; James et Canérot, 1999; Canérot et al., 2005) but only local small structures have been so far described with detail (Lenoble and Canérot, 1992; Canérot and Lenoble, 1993). The present study is based on original field investigations complemented by well log data and a new interpretation of a seismic reflection profile for the northern part of the area. The results of the study are illustrated by four new balanced cross-sections of representative transects of the Chaînons Béarnais belt, detailed mapping of key sectors, and a sequential restoration of the tectono-sedimentary evolution during the rift opening and subsequent inversion. We propose that the fold-thrust deformation observed in the pre- and syn-rift strata is not only related to the Pyrenean shortening, but also was largely achieved through salt tectonics, involving diapirism and possibly gravity-induced contraction, during the Mesozoic rifting. We discuss the differences between this interpretation and previous works that reported the salt structures of the western Pyrenees as autochthonous diapirs presently above basement normal faults relict from the former continental margins (Canérot, 1988, 1989; James and Canérot, 1999; Canérot et al., 2005).

2. Geological setting

2.1. Tectonic framework of the Pyrenean mountain belt

After the Variscan orogeny that shaped the Paleozoic basement of the Pyrenees (Cochelin et al., 2017, and references therein), different episodes of rifting took place during the Permian, the Triassic and the Cretaceous. While Triassic extension has been reported, to which thick evaporites were associated (Biteau et al., 2006; Ortí et al., 2017; Soto et al., 2017), the main rifting stage in the Pyrenean realm occurred in the early and mid-Cretaceous, leading to the main basin opening episode precursor to the inversion and mountain building. The mid-Cretaceous rifting in the Pyrenean realm was related to the opening of the Bay of Biscay oceanic basin located more to the west and involved a major episode of crustal stretching, basin subsidence and mantle exhumation during the Albian-early Cenomanian (Lagabrielle and Bodinier, 2008; Jammes et al., 2009; Lagabrielle et al., 2010; Mouthereau et al., 2014; Tugend et al., 2014; Teixell et al., 2016, 2018; Grool et al., 2018; Espurt et al., 2019). Most of the inverted rift system now corresponds to the so-called North-Pyrenean Zone (NPZ; Fig. 1), where rifting-related features comprise 1) syn-rift Albian-lower Cenomanian flysch basins (the Black Flysch Group; Souquet et al., 1985), 2) peridotite bodies (the lherzolites from their type area in the central Pyrenees) originating from the exhumed mantle and included in the Mesozoic series (Lagabrielle and Bodinier, 2008; Jammes et al., 2009; Lagabrielle et al. 2010; 2019a and b; Corre et al., 2016), 3) alkaline magmatic bodies (Montigny et al., 1986), and 4) a HT-LP metamorphim of the Mesozoic series, dated from the Albian to the Coniacian (for magmatism and metamorphism, see a review and references in Clerc et al., 2015). An unconformity in the lower Cenomanian coinciding with a widening of the basin is often considered as marking the transition to a post-rift stage (e.g. Debroas, 1987, 1990). However, there is no consensus in the literature on the kinematics of the North-Pyrenean rifting, which has been interpreted either in a sinistral strike-slip (Choukroune and Mattauer, 1978; Debroas, 1987, 1990; Canérot, 2017) or in a near orthogonal extension context (Jammes et al., 2009; Masini et al., 2014; Tugend et al., 2014; Saspiturry et al., 2019), due to the lack of robust geological evidence and a controversial plate kinematic framework (Bronner et al., 2011, Barnet-Moore et al., 2016; Nirrengarten et al., 2018, and references therein).

The Pyrenean orogenic shortening spanned from the late Santonian (circa 84 Ma) to the early Miocene (circa 20 Ma). First it involved the tectonic inversion of the rift system and subduction of the exhumed mantle tract, and then the formation of the south-vergent crustal accretionary prism corresponding to the Axial and South-Pyrenean Zones (Fig. 1), formed after the Iberian upper continental margin in relation to the northward subduction of the Iberian lower crust and lithospheric mantle (Jammes et al., 2009; Mouthereau et al., 2014; Tugend et al., 2014; Teixell et al., 2016, 2018; Grool et al., 2018; Espurt et al., 2019). Recent interpretations depict the inversion of the rift system as a pop-up structure where the North-Pyrenean Fault and Lakora thrust correspond to the south-vergent southern edge of the pop-up, subsequently verticalized during stacking of thrust units in the Axial Zone, while the North-Pyrenean Frontal Thrust (NPFT) corresponds to the north-vergent northern edge over the Aquitaine foreland basin (Lagabrielle et al., 2010; Mouthereau et al., 2014; Teixell et al., 2016, 2018; Espurt et al., 2019) (Fig. 1).

2.2. The North-Pyrenean Zone in the Chaînons Béarnais area

2.2.1. General structure

The Chaînons Béarnais belt (CBB) corresponds to a 50 km-long segment of the west-central NPZ, constituted by a system of E-W trending Jurassic to Aptian carbonate anticlinal or thrust ridges cored by Middle-Upper Triassic rocks (mainly Keuper facies shales at the surface), and separated by synclines with thick uppermost Aptian to lower Cenomanian marl and flysch deposits (Fig. 2). To the west and east, the CBB ridges plunge laterally below the Albian-Cenomanian flysch of the so-called Mauléon and Ossun basins, respectively.

To the north, the CBB is bounded by the North-Pyrenean Frontal Thrust (NPFT). The Rébénacq transverse fault zone (Fig. 2) separates an eastern segment where the NPFT is emergent at the surface, and a western segment where this thrust is a blind structure marked at the surface by the km-scale Oloron anticline. North of the NPFT, the Aquitaine foreland basin comprises thick depocenters of Upper Cretaceous flysch sequences and Tertiary strata covered by post-orogenic Upper Miocene to Quaternary molasse.

To the south, the CBB lies above a system of small thrust sheets, here named the Bedous-Laruns thrust units (BLTU), forming the northern edge of the Axial Zone and mainly comprising Upper Paleozoic strata (Silurian to Carboniferous) with a Lower Triassic sandstone tegument (Canérot et al., 2001). Local remnants of Middle-Upper Triassic shales, carbonates and ophite, and Aptian-Albian limestones and conglomerates are occasionally preserved in these thrust sheets. To the west, the Iguntze massif corresponds to the western extension of the BLTU, with a thick sequence of Albian conglomerates (the Mendibelza conglomerates) onlapping the Paleozoic basement (Boirie and Souquet, 1982). The contact between the CBB and BLTU corresponds to the western extension of the North-Pyrenean Fault. Between the Aspe and Ossau valleys (Fig. 2), the Bergon and Tacha klippes correspond to the southernmost remnants of the CBB Mesozoic succession resting on the BLTU. In the western area, the Iguntze massif and BLTU are thrust southwards by the Lakora-Larra thrust system over the

Upper Cretaceous carbonates and flysch covering the Paleozoic of the Axial Zone (Teixell, 1990, 1996). The Lakora-Larra thrust system passes eastwards to the Eaux-Chaudes - Eaux-Bonnes thrust system, which extends eastward into the basement of the northern Axial Zone (Labaume et al., 2016).

The Iguntze massif-BLTU and the southern part of the CBB correspond to the former Iberian margin of the Pyrenean rift, while the northern CBB (Mail Arrouy ridge; Fig. 2) are ascribed to the European margin (Canérot et al., 1978; Puigdefàbregas and Souquet, 1986; Combes et al., 1998; Tugend et al., 2014; Teixell et al., 2016). In the eastern CBB, a small domain of scapolite-bearing Kimmeridgian marble occurs at the center of the Tres Crouts structure (Casteras et al., 1970a) (Fig. 2), comparable to other occurrences of the Cretaceous North-Pyrenean metamorphic zone further east (the so-called Internal Metamorphic Zone) which delineate the axis of the mid-Cretaceous rift (Clerc et al., 2015). The rift axis is also identified by the occurrence of seven lherzolite bodies, most of them located along the CBB axis (Fig. 2). Recent studies show that high paleo-temperatures in the CBB are not restricted to the Tres Crouts structure, but that most of the belt was affected by peak temperatures around 350°C, with local maxima between 400 and 500°C close to some of the lherzolite bodies and in the Tres Crouts metamorphic domain (Clerc et al., 2015; Menant et al., 2016; Villard, 2016; Corre, 2017; Ducoux, 2017).

2.2.2. Stratigraphy of the Mesozoic-Cenozoic

A general description of the stratigraphy in the CBB area can be found in the BRGM geological maps and notices (Alimen et al., 1963; Casteras et al., 1970a and b; Ternet et al., 1980, 2004) and is summarized in the stratigraphic column in Figure 3.

Most of the rocks exposed in the CBB correspond to the Mesozoic sedimentary cover, beginning with the Middle-Upper Triassic deposits. The latter consist of a disorganized association of the characteristic shale/evaporite Keuper facies and occasional bodies of the Muschelkalk facies, and also contain tectonic breccia (cargneule) and frequent intrusive ophite bodies. Except local gypsum occurrences, evaporites are most often absent in outcrop due to dissolution, but more than 2620 m of evaporite-rich facies, mostly halite, were drilled without reaching their base in the Bélair well (cf. well log in http://infoterre.brgm.fr/), in the hanging wall of the NPFT (BEL1 in Fig. 2). For convenience in the following, we collectively refer to the Middle-Upper Triassic complex as Keuper according to its main component.

Over the Triassic is a series of platform carbonates of Jurassic – Early Cretaceous age, 1500 to 2000 m-thick when complete (Lenoble, 1992; James, 1998). The Jurassic corresponds to a westward-facing carbonate ramp interpreted as formed in a context of moderate E-W trending extension, while the Neocomian records the formation of the E-W-trending structures of the Pyrenean rift (Lenoble, 1992; James, 1998, James and Canérot, 1999; Canérot et al., 2005). The Lias usually begins with a polygenic breccia reworking various carbonate facies, followed by dolomites and limestones passing upward to black marls. The Dogger comprises Bajocian-Bathonian limestones followed by an about 400 m-thick interval of black dolomite of Bathonian-Callovian age (referred to below as the Dogger dolomite). Above a reduced dolomitic or calcareous Oxfordian, the Malm comprises Kimmeridgian limestones with marl intervals, followed by a Portlandian dolomite.

The Lower Cretaceous begins by a discontinuous alterite horizon, up to ten of meters thick, comprising ferruginous, locally pisolitic, breccia, sandstone and clay ("bauxite") which traduces transient emersion associated to a karstic erosion surface in the Upper Jurassic (Lenoble, 1992; Combes et al., 1998; Canérot et al., 1999). The return of marine conditions is marked by Barremian limestones and marls. They are followed by lower Aptian (Bedoulian) marls (the Sainte-Suzanne marls) overlain by an about 300-400 m-thick layer of reefal to peri-reefal limestones (Urgonian facies). These limestones are mostly upper Aptian (Gargasian) in age but locally extend to the uppermost Aptian (Clansayesian) to lower Albian. Locally, the erosion of the Jurassic reaches deeper stratigraphic levels and the Neocomian hiatus is wider, in particular in the SW area where the Urgonian limestones rest on the Dogger dolomite and in the Asasp diapir (Fig. 2) where it rests on Keuper facies (Casteras et al., 1970b).

The upper (Clansayesian-lower Albian) part of the Urgonian limestones shows lateral transitions to argillaceous limestones and marls (the so-called Spicule marls, or Haux marls in Souquet et al., 1985) which finally cover the limestone units, marking the onset of platform drowning and basin deepening around the Aptian-Albian boundary. Above, the rapid subsidence of the mid-Cretaceous basin during the main rifting stage is registered by the middle Albian to lower Cenomanian black marls and turbidites of the Black Flysch Group (Roux, 1983; Souquet et al., 1985), at least 2000 m thick. To the south, the lateral equivalents of the Black Flysch in the BLTU correspond to small, mainly carbonate massifs in the eastern area (Gallagos, Bazès, Arbéost, located in Fig. 2) and to the middle-upper Albian Mendibelza conglomerates in the west (Iguntze massif) (Boirie and Souquet, 1982). The latter rework mainly Paleozoic metasediments, as well as Permian-Triassic sandstones and Albian platform carbonates.

The Black Flysch is followed by the Upper Cretaceous flysch sequences which are preserved from erosion only in the NW part of the CBB and in the southern Aquitaine Basin. These comprise about 2000 m of Cenomanian to Santonian calcareous flysch (Roux, 1983) which exhibit the lower Cenomanian unconformity at the base in the Asasp area (Casteras et al., 1970b) (Fig. 2). These are followed by up to 3000 m of Campanian-lower Maastrichtian sandy flysch and upper Maastrichtian marls (Serrano, 2001; Biteau et al., 2006; Serrano et al., 2006), which correspond to the first syn-orogenic deposits. The Tertiary, present only in the Aquitaine Basin, begins with 80-100 m of lower Paleocene pelagic limestones followed by middle Paleocene to Ypresian clays and sands, which are the last flysch facies (ibid). These are covered by a west-prograding system of coastal sandstones and offshore marls of Ypresian to lower Lutetian age, followed in turn by the upper Lutetian to Oligocene molasse recording terrestrial environments in the upper part. The succession of the Aquitaine basin ends with post-orogenic Upper Miocene to Quaternary detrital sediments.

2.2.3 Basement and magmatic rocks

Pre-Keuper rocks outcrops are scarce in the CBB and comprise mantle rocks (more or less serpentinized lherzolite), Paleozoic meta-sediments, and a tegument of Lower Triassic sandstones. Six lherzolite bodies occur along the axial part of the CCB, generally associated with lenses of Paleozoic or Lower Triassic rocks. Five of them are embedded in Keuper rocks at the core of anticlines (Tos de la Coustette, Moncaup, Saint-Pé) or thrust hanging walls (Saraillé, Turon de la Técouère), while the Urdach lherzolite body is covered by the upper Albian breccias and flysch at the western termination of the Mail Arrouy thrust sheet (Fortané et al., 1986; Jammes et al., 2009; Debroas et al., 2010; Lagabrielle et al., 2010, 2019b; Corre, 2017) (Fig. 2). In the northeastern area, several hm- to km-scale bodies of Silurian-Devonian metasediments, some of them covered by Lower Triassic sandstones, occur along the emerging branch of the NPFT at the base of the hanging wall sequence (Fig. 2). These basement bodies are directly covered by Aptian limestones, and one of them overlies a lherzolite body (Montaud).

Small bodies of Upper Cretaceous alkaline magmatic rocks occur in the northern part of the CBB. They correspond to intrusive sills and dykes and submarine lava flows (pillow lavas) intercalated mainly in the Black Flysch.

3. Cross-sections of the North-Pyrenean Zone in the Chaînons Béarnais area

We present four new cross-sections of the NPZ in the CBB area (Fig. 4), constructed from original field observations and structural data complemented by stratigraphic data from previously published maps (Alimen et al., 1963, Canérot, 1964; Paris, 1969; Casteras et al., 1970a and b; Ternet et al., 1980, 2004; Roux, 1983; Souquet et al., 1985). The subsurface structures of the NPFT area were constructed from stratigraphic logs of oil exploration wells and, for cross-section 4, from a new interpretation of an industrial seismic profile (see references below, Section 4.3.1). The Move software was used at some steps of cross-section construction. Below, we outline first the major features of the cross-sections. More detailed descriptions and inferences from key-areas featuring salt structures are provided below in Section 4.

3.1. Structure of the Mesozoic cover

We interpret that the CBB is a fold and thrust system decoupled from the Paleozoic basement along the Keuper unit which cores the anticlines. The Keuper thickness at antiformal cores is variable, many of them showing reduced thickness or disappearance or apparent faulting indicative of salt squeezing and welding. A characteristic of the CBB structure is the lack of consistent structural vergence, a feature typical of fold-thrust belts detached above thick salt (Davis and Engelder, 1985; Hudec and Jackson, 2001). In the west (cross-sections S1 to S3 in Fig. 4), the northern and central ridges (Mail Arrouy and Sarrance, respectively) show south-vergent thrusts (Fig. 5) (the Sarrance thrust anticline passing eastward to the south-vergent Aran anticline), somewhat unexpected in the North-Pyrenean retrowedge, while the southern ridge (Layens-Ourdinse) corresponds to a north-vergent syncline-anticline pair. The Bergon klippe, the southernmost occurrence of the CBB, features also a north-vergent syncline (cross-sections S2 and S3 in Fig. 4). In the east (cross-section S4 in Fig. 4), the northern Saint-Pé anticline is an upright structure, the central Tres Crouts structure features two synclines of opposite vergence, and the southern Estibète-Pibeste ridge is thrust southwards along the NPF. The Andorre syncline, between the Tres Crouts structure and the Estibète-Pibeste ridge, is an upright structure in cross-section S4 but it features a northward vergence both east and west of the section. The tectono-sedimentary relationships in the Mesozoic series of the CBB, involving bed fanning and thickening in the synclines (growth strata) and lateral facies changes, are discussed in Section 4.

Most of the stratigraphic formations of the CBB succession feature a bedding-parallel foliation hereafter referred to as S0-S1. It corresponds to a slaty cleavage in the marly/pelitic layers (Fig. 5b), and to a schistosity marked by a grain-shape fabric of calcite in limestones (Fig. 5c). The intensity of the S0-S1 is heterogeneous both laterally and vertically, and it is absent in the dolomites. A later S2 is locally present with variable attitudes, probably related to local deformation zones. The S0-S1 is attributed to the mid-Cretaceous syn-metamorphic extensional context (Corre et al., 2016; Villard, 2016; Corre, 2017), although describing and discussing the distribution of these cleavages is beyond the scope of this paper. It must be noted that no widespread oblique regional cleavage related to the Pyrenean compression can be observed.

3.2. The basement of the Chaînons Béarnais Belt

Cross-section construction implies a difference of elevation of the Paleozoic basement top under the CBB of about 8000 m, from its outcrop area in the south to its deepest occurrence below the northern CBB (Fig. 4). This basement is interpreted as the distal part of the former Iberian margin of the Pyrenean rift, now forming the hanging wall of the NPFT (Teixell et al., 2016, 2018), but its internal fault structure remains largely unconstrained. The geometry of the cover structures above (tight folds and thrusts) suggests décollement in the Keuper (Fig. 4), the Mail Arrouy thrust being the only one with a kilometric displacement. On the other hand, there is no evidence for large normal-faulted tilted blocks involving the Paleozoic basement and its Mesozoic cover similar to the Arbailles block of the neighbouring Mauléon basin (Ducasse et al., 1986; Canérot, 1989; Masini et al., 2014; Saspiturry et al., 2019). Hence, we favor the interpretation of a general decoupling between the CBB fold-and-thrust cover and the underlying basement. We infer a relatively smooth basement top affected by thrusts faults branching to the Keuper décollement level above. To the south, the thrust structures correspond to the northern part of the south-vergent BLTU, while to the north, we infer north-vergent thrusts in the nearest hanging wall of the NPFT. The occurrence of inherited normal faults with limited offset is also possible, but there is no evidence that some of them were inverted as reverse faults breaching up to the surface as shown in some published cross-sections (Canérot, 1989; Dubos-Salée et al., 2007). In order to minimize the Keuper volume during section construction, our sections show primary welding of the deepest synclines to the basement top.

3.3. The structures south of the CBB: the Iguntze-Mendibelza massif, Bedous-Laruns thrust units and Axial Zone

To the south-west, the CBB is in contact with the easternmost part of the Iguntze massif by the steeply-dipping Licq fault (cross-section S1 in Fig. 4). The Iguntze massif comprises the middle-upper Albian Mendibelza conglomerates onlapping southwards a slice of Paleozoic metasediments (much reduced on cross-section S1). Based on the onlap geometry (Boirie and Souquet, 1982) and the frequent remnants of the Permian-Lower Triassic sandstone tegument preserved along the onlap surface (Casteras and Souquet, 1970), we follow the interpretation of the latter surface as the northward tilted basement top (Teixell, 1993; Teixell et al., 2016; Saspiturry et al., 2019) rather than as the denuded footwall of an intracrustal detachment associated to southward-tilted basement fault blocks (Johnson and Hall, 1989; Masini et al., 2014). The Iguntze massif and Licq fault have been hypothetically shown south of the Bergon klippe on cross-sections S2 and S3. From its main exposure west of the study area, the Paleozoic slice of the Iguntze massif is interpreted as detached by the short-cut of a former normal fault footwall by the Pyrenean thrust (Teixell, 1993). This differs from alternative interpretations rooting the Iguntze-Mendibelza thrust in the underlying crustal basement (e.g. Masini et al., 2014; Dumont et al., 2015), which do not match the observed low-angle geometry of the thrust above a footwall of Keuper facies and branched to the north to the Licq fault (Casteras and Souquet, 1970).

In cross-section S1, the southern CBB and Iguntze massif are thrust above the Bedous Triassic unit, comprising Keuper facies, Muchelkalk carbonates and ophite bodies, itself thrust above the Upper Cretaceous cover of the Axial Zone. The two thrusts branch southward into the Lakora thrust, defining the Bedous Triassic unit as a duplex structure, while a lower branch, the Larra thrust, propagated near the top of the Upper Cretaceous carbonates. Both the Lakora and Larra thrusts propagated southward up to the Tertiary succession of the northern Jaca basin and were subsequently folded by the Axial Zone antiform, here corresponding to the Gavarnie thrust hanging wall culmination (Teixell, 1990, 1996; Labaume et al., 2016; Labaume and Teixell, 2018).

East of the Gave d'Aspe valley, the southern CBB rests over the Paleozoic basement and Lower Triassic sandstone tegument of two of the BLTU: the Bois de la Traillère and Montagnon d'Iseye thrust units in cross-sections S2 and S3, respectively (Fig. 4). In cross-section S3, the Montagnon d'Iseye unit is itself thrust (with intervening discontinuous slices of the Bedous Triassic) above the Eaux-Chaudes km-scale recumbent fold-thrust structure involving the Paleozoic metasediments and their cover of Upper Cretaceous limestone and flysch (which corresponds to the northernmost structure of the Axial Zone; Caldera et al., 2019). A western extension of the Eaux-Chaudes thrust-fold is shown tentatively in cross-section S2. All these thrust units branch southward into the Lakora and Larra thrusts. Hence, the southern CBB décollement, Iguntze massif, Bedous Triassic unit, BLTU and the Eaux-Chaudes fold-thrust form a complex south-vergent duplex structure corresponding to the exhumed root of the Lakora and Larra thrusts. Steep north-vergent reverse faults in the Axial Zone basement correspond to small backthrusts in the Gavarnie thrust hanging wall that deform the previous low-angle Lakora-Larra thrust system (Dumont et al., 2015).

3.4. The structure north of the CBB: Grand-Rieu High and North-Pyrenean Frontal Thrust

North of the hanging wall cut-off of the basement top by the NPFT, the Grand-Rieu High (cross-sections S1 and S4 in Fig. 4) corresponds to a basement horst identified in seismic profiles and wells (Bourrouilh et al., 1995; Serrano et al., 2006). It is a mid-Cretaceous structure that separates the Chaînons Béarnais and Mauléon basins in the south from the Arzacq-Tarbes basin in the north, and is interpreted to correspond to the upper European margin of the Pyrenean rift (e.g. Lagabrielle et al., 2010; Masini et al., 2014; Teixell et al., 2016; Saspiturry et al., 2019). The frontal part of the NPFT cuts the Mesozoic cover above the Grand Rieu High as a blind thrust in the west and emerging in the east (cross-sections S1 and S4 in Fig. 4, respectively).

The structure of the NPFT in cross-section S1 is deduced from surface geology (Alimen et al., 1963; Casteras et al., 1970b), from four well logs located along the section (OLN1, CAD2, FLAS2 and LRT1; see location of OLN1 and CAD2 on map in Figure 2, and logs in Supplementary Data, Fig. S1), and the cross-section published by Lagabrielle et al. (2010). The major structure is the large north-vergent Oloron anticline, cored by a thick accumulation of Keuper facies. This interpretation accords with the thick accumulation of Keuper facies drilled 11 km to the east in the Bélair well (cf. above, Section 2.2.2) below the Jurassic of the hinge zone of the Oloron anticline (see the corresponding cross-section in Biteau et al., 2006). The northern limb of the Oloron anticline comprises a thick growth strata fan of Campanian-Maastrichtian flysch and overlying Paleocene-Eocene flysch and shallow marine deposits. On the southern Grand-Rieu High, the Jurassic-Lower Cretaceous strata were totally removed and the Cenomanian to Santonian flysch is also absent. The Upper Cretaceous begins with a few tens of meters thick breccia layer resting on the Keuper facies (well CAD2) or on the Lower Triassic Buntsandstein facies that overlies Paleozoic metasediments (well LRT1). The breccia reworks Paleozoic metasediments, Buntsandstein sandstone and Jurassic to Lower Cretaceous carbonates, and is onlapped by the Campanian flysch (Supplementary Data, Fig. S1). The occurrence of Keuper bodies along the upper branch of the NPFT is discussed below (Section 4.3.1).

In cross-section S1, a lower branch of the NPFT propagated 16 km northward along the base of the Upper Cretaceous flysch to form the Pau anticline, which is the northernmost structure of the North-Pyrenean front (see Figure 5 in Lagabrielle et al., 2010). It features isopach beds in the Upper Cretaceous and growth strata in the Eocene (see Figure 9 in Canérot et al., 2005).

The structure of the NPFT in cross-section S4 (Fig. 4) is constrained by the combination of stratigraphic and structural data from the surface exposure, two well logs (SVT1 and LVN1; see location of wells on map in Figure 2, and logs in Supplementary Data, Figure S1), and the LR5 seismic profile published by Serrano et al. (2006) (see interpretative line-drawing and comments in Supplementary Data, Fig. S2). The seismic image was converted to depth using the time/depth conversion in wells and isohypse maps of key stratigraphic surfaces in Serrano et al. (2006). In cross-section S4, the NPFT separates the northern limb of the Forêt de Mourle syncline in the hanging wall from a large northward overturned syncline in the footwall. The hanging wall features a body of Paleozoic metasediments covered by Aptian limestones and the Albian Black Flysch. The Paleozoic corresponds to one of the bodies that occur discontinuously at the hanging wall of the NPFT in the eastern area, and it overlies the Montaud lherzolite body located 2 km west of the section (Fig. 2). The footwall syncline comprises the Cenomanian to Eocene succession, with a large growth strata fan in the Campanian to Eocene. In the SVT1 well, the Upper Cretaceous flysch rests on a few tens of meters of Neocomian carbonates and shales following the Keuper and Buntsandstein facies and Devonian metasediments of the Grand-Rieu High. More to the north, the Campanian flysch onlaps an erosion surface cutting the Albian flysch of the Tarbes basin, and the Albian flysch rests itself on an erosional surface cutting the Jurassic. Due to the presence of a slight anticline in the Upper Cretaceous more to the north (see the complete LR5 seismic profile in Serrano et al., 2006), we interpret that the base of the Upper Cretaceous flysch acted as a Pyrenean thrust décollement surface, similarly to the structure observed more to the west (cross-section S1 in Figure 4). The occurrence of Keuper bodies along the upper branch of the NPFT and the origin of the erosional surfaces are discussed below (Section 4.3.1).

4. Salt tectonics in the Chaînons Béarnais belt

Salt diapirs formed during the Cretaceous extension and subsequently squeezed during the Pyrenean compression have already been described in the Aquitaine basin and adjacent Mauléon basin in the frame of intensive oil exploration (Mediavilla and Mauriaud, 1987; Bourrouilh et al., 1995; Canérot et al., 2005; Biteau et al., 2006; Serrano et al., 2006). A diapiric origin of the CBB anticlines with halokinesis initiated during the Early Cretaceous was first proposed by Canérot (1988), based on succinct description of thickness reduction of the Barremian-Aptian carbonates at anticline hinges, locally associated to erosional surfaces, and lateral facies transitions between the Aptian carbonates and marls deposited in the adjacent synclines. In particular, Canérot (1988) notes the unconformity between the Barremian and Jurassic carbonates at the Moncaut anticline crest (Figs. 2 and 6). Canérot (1989) and James and Canérot (1999) provide more detailed descriptions and kinematic restorations of Lower Cretaceous diapirs in the Mauléon basin. On the other hand, detailed description in terms of salt structures in the CBB remain limited to a transverse welded diapir in the Lourdios syncline (Lenoble and Canérot, 1992) (“Ponsuzon weld” in Fig. 7), and the Lauriolle breccia (located at the eastern extremity of the Ourdinse ridge, Fig. 7), interpreted as related to diapir collapse

(Canérot and Lenoble, 1993). According to these various papers, the diapirs formed above basement normal faults bounding tilted blocks of the Cretaceous rift and remained there, squeezed during the subsequent Pyrenean orogeny without major décollement from their Paleozoic substratum. Canérot et al. (2005) further develop description of diapirism in the Aquitanian domain, including the interpretation of the NPFT as a former Cretaceous diapiric ridge inverted by the Pyrenean compression.

In what follows we present a new description of a selection of characteristic salt structures in the CBB and discuss the timing and context of their development. We first present the south-western part of the CBB, which provides the largest exposure of the late Aptian-Albian basins, then we describe the complex Tres Crouts structure which bears evidence of a protracted development in several stages, and finally we examine the structures related to the Pyrenean inversion, in particular the NPFT.

4.1. The Lourdios and Barescou minibasins and adjacent salt ridges

The area comprises two depocentrers of upper Aptian-Albian marls and flysch, bounded by Jurassic-Lower Cretaceous carbonate ridges, from south to north: the Lourdios syncline between the Layens-Ourdinse ridge and the Sarrance-Aran anticline, and the Barescou syncline between the latter anticline and the Mail Arrouy thrust ridge (Figs. 2 and 7). The map in Figure 7 is based on original mapping in the field and 3D aerial photographs. Although the overall structure of the area was correctly reported in previous maps (Canérot, 1964; Paris, 1969; Casteras et al., 1970b; Haller and Jardiné, 1986; Ternet et al., 2004), our mapping provides new structural data, more precision, and new interpretation for numerous contacts, in particular for the southern limb of the Sarrance anticline (including the lherzolite massifs) and for the eastern Lourdios syncline (regarding the map pattern and stratigraphic correlation of limestone-marl intercalations in the Pic Montagnon and Ourlène areas).

4.1.1. The Layens-Ourdinse carbonate ridge: welded diapirs and overturned megaflaps

The stratigraphy of the Layens-Ourdinse ridge is characterized by a deep Neocomian erosion and associated hiatus, with the upper Aptian Urgonian limestones resting on the Dogger dolomite which often displays an alterite horizon at its top. The structure corresponds to a recumbent syncline-anticline pair with northward vergence (cross-sections S1 to S3 in Fig. 4, and Fig. 7). The antiform structure is preserved from erosion at the Layens summit (Fig. 8) and Ourdinse plateau (Fig. 9) where it can be observed that it corresponds to a quasi-welded overhang of Keuper facies above a sub-horizontal overturned megaflap of Jurassic and Urgonian carbonates. In the Layens, transverse structures interfere with the general E-W trend, i.e. N-S trending folds in the western slope of the Aspe valley and the NNE-SSW-trending megaflap on the eastern flank of the Layens summit (Fig. 8). The Urgonian limestones are about 350 m thick in the normal limb of the syncline and thins dramatically across the syncline hinge to pass to less than 100 m in the megaflap (cross-sections S1 to S3 in Fig. 4), attesting diapir rise during the late Aptian.

4.1.2. The Sarrance and Aran anticlines: squeezed salt walls and salt extrusion

The Sarrance anticline is cored by the Keuper facies (cross-section S1 in Fig. 4, and Fig. 7). Two lherzolite bodies, the Saraillé and Tos de la Coustette lherzolites, along with bodies of Paleozoic metasediments, show lateral contacts with the Keuper and are covered by the Jurassic carbonates which show there a subtractive contact at the base (Fortané et al., 1986; Corre et al., 2016; Corre, 2017; Lagabrielle et al., 2019a). The stratigraphy of the

Sarrance anticline is more complete than in the Layens-Ourdinse ridge, with the northern limb comprising the Kimmeridgian and Neocomian carbonates (the latter disappearing westward according to Lenoble, 1992), Sainte-Suzanne marls and thick (350-400 m) Urgonian limestones. Nevertheless, this succession thins in the southern limb with strong reduction of the Kimmeridgian by erosion, absence of the Neocomian and reduced thickness of the Urgonian limestones (100-150 m). This reduced Urgonian is thinner than in the normal limb of the Layens-Ourdinse syncline, which also indicates rise of the Sarrance ridge in late Aptian times. The Sarrance ridge has an upright geometry with vertical northern limb. The central part of the southern limb features a sub-horizontal south-vergent thrust carrying the Keuper facies and the Saraillé massif above the Spicule marls of the Lourdios syncline with a displacement not exceeding 1 km. The Saraillé massif comprises a south-vergent recumbent anticline of Mesozoic carbonates wrapping in its core the Saraillé lherzolite and a lens of Paleozoic metasediments (see Corre et al., 2016, Corre, 2017, and Lagabrielle et al., 2019a for detailed description). East of the thrust unit, both flanks of the Sarrance ridge are welded with an overturned southern flank. To the west, the southern flank features sub-vertical to steep southward dips. The Tos de la Coustette lherzolite prevented welding, but the lherzolite is bounded by a tear fault west of which the anticline extremity is welded.

The structure of the thrust unit rooted in the anticline core and the lateral welding of the anticline denote a salt extrusion related to salt wall squeezing and that carried part of the anticline crest (the Saraillé massif). Furthermore, the Sarrance ridge shows two peculiar structural features that we interpret as also resulting from the salt wall deflation during salt expulsion from its core: i) on both sides of the thrust unit, the carbonates and overlying Spicule marls of the southern flank curve toward the north until their cut off at the thrust, and ii) north of the thrust unit, the northern flank features a reentrant accommodated by sub-vertical N-S trending faults (Fig. 7). The Spicule marls in the southern flank of the Sarrance anticline dip southward, but with lower values in the thrust footwall than more to the west (Fig. 7), which may also have resulted from evacuation of underlying salt. These structures are quite analogous to those on several salt anticlines of the Zagros fold belt in SW Iran that feature salt glacier extrusions associated with forelimb curvatures and cut-offs and back-limb reentrants similar in style and dimensions to those at Sarrance (Jackson and Hudec, 2017).

To the east, a complex transverse fault zone makes the lateral transition between the Sarrance and Aran ridges, with offset of their axes (referred to as the Aran transverse fault zone in the following and labelled ATFZ in Fig. 7). The Aran anticline has been less exhumed, with discontinuous surface exposition of Urgonian limestones covered by the Spicule marls. The Aran is a tight anticline with steeply dipping limbs, the narrow shape of which suggesting the absence of the Jurassic-Neocomian in the core. We interpret this structure as an ancient exposed diapir where the Urgonian limestones deposited directly on the Keuper before being finally squeezed. Some limestone beds at the top of the Urgonian succession pinch out in the Spicule marls in the southern limb of the anticline (cross-sections S2 and S3 in Fig. 4, and Figs. 7 and 10), attesting its rising at late Aptian times.

4.1.3. The Lourdios syncline: a Clansayesian (-lower Albian) minibasin

The Lourdios syncline shows marked stratigraphic differences between its western and eastern parts. While the area located west of the Aspe river shows the classical superposition of the Spicule marls above the Urgonian limestones, the eastern area (Bois de Gey, Pic Montagnon) features numerous intercalations of Urgonian-type limestones in the marls (Fig. 7). The BRGM map (Casteras et al., 1970b) ascribes an Albian age to the lowest layer of Spicule marls, and an upper Aptian age to the overlying marl-limestone intercalations, implying a thrust between both (see also Canérot et al., 1999). Conversely, our field observations and mapping confirm the stratigraphic continuity of the marl-limestone intercalations with the underlying Urgonian limestones from the Aran anticline crest to the Ourdinse overturned flap as was originally shown in Canérot (1964). Lenoble (1992) attributed a Gargasian age to the main Urgonian limestones and an uppermost Aptian (Clansayesian) age to the overlying marl-limestone intercalations, possibly reaching the Albian in the upper part. Stratigraphic continuity implies that a large part of the Spicule marls in the western part of the syncline has also a Clansayesian age.

The Lourdios syncline infill features a growth pattern. Synsedimentary folding with a pouch-like geometry is best evidenced east of the Aspe river thanks to the marl-limestone intercalations which show a growth pattern on both limbs (Bois de Gey-Pic Montagnon area; cross-sections S2 and S3 in Fig. 4, and Figs. 7, 9 and 10). To the north, the lower marl beds feature a fan-geometry against the southern limb of the tight Aran anticline. To the south, the marls and intercalated limestone beds thin southwards when passing into the overturned flap of the Ourdinse ridge. The along-strike thickness variations also evidence for depocenter shifting probably related with transverse structures, with the maximum thickness (a hundred of meters) of the lowest limestone bed in a depocenter at the west of the Montagnon mountain while the upper beds merge eastward in the 200 m thick carbonate mass forming the Pic Montagnon (Fig. 7).

West of the Aspe river only the lowest of the intercalated limestone beds is present, which onlaps southwards the Urgonian limestones of the Layens ridge (Fig. 7), giving a growth strata pattern similar to that described to the east. The western Lourdios syncline contains mostly a thick accumulation of argillaceous limestones, marls and rare thin-bedded silt to fine-grained sandstone layers all corresponding to the Spicule marls unit (Souquet et al., 1985). In the western part (cf. near the village of Lourdios-Ichère; Fig. 7), the syncline is strongly asymmetric with a wide northern limb where a slight southward dip reduction traduces a growth strata arrangement, and a very short southern limb against the steep Urgonian limestones of the Layens megaflap (cross-section S1 in Fig. 4). This growth geometry indicates a progressive depocenter migration, likely by salt expulsion. North of the Lourdios-Ichère village, the lower part of the succession contains several debris flow beds reworking clasts of bioclastic limestone. On the other hand, the Spicule marls present in the Saraillé thrust unit has a more carbonated facies than the marls of both limbs of the ridge. This thrust unit representing an element of the Sarrance anticline crest, we can infer that the anticline crest at Clansayesian times was a rising high where shallower bathymetry allowed carbonate deposition feeding the debris flows in the adjacent deeper domain. Isolated limestone lenses, up to a few tens of meters long occur in the eastern part of the western Lourdios syncline, which may represent olistoliths originating either from the northern (Sarrance) or southern (Layens) rising highs.

On the western side of the Aspe valley, an alignment of blocks of Triassic carbonates and breccias defines a N-S trending welded diapir across the Lourdios syncline (Lenoble and Canérot, 1992) ("Ponsuzon weld" in Fig. 7). This diapir collapsed the western compartment while the top of the Urgonian limestones crops out in a small anticline on the eastern side. It may have contributed to the salt evacuation discussed above for the Saraillé thrust unit. A steeply dipping fault affects the Gargasian limestone and overlying marls at the syncline core zone with a hundred of meters displacement, which we interpret as an ancient normal fault, inverted as a reverse fault in the Aspe valley (cross-sections S2 and S3 in Fig. 4, and Figs. 7, 9 and 10).

We underline that the stratigraphic continuity across the Lourdios syncline shown in the present work does not favor the existence of a large-displacement south-vergent thrust at the base of the Sarrance anticline and emerging in the syncline as suggested in a previous work (Tugend et al., 2014).

4.1.4. The Ourlène carbonate ridge and Barescou syncline: a Clansayesian-Albian depocentre

In the northern limb of the Aran anticline, the Spicule marls covering the Gargasian limestones are themselves covered by the Urgonian limestones of the Ourlène ridge (cross-sections S2 and S3 in Fig. 4, and Fig. 7). In the eastern part, the ridge features a complex stratigraphic pattern with marl intercalations, carbonate pinch-outs, erosional truncations and onlaps. Locally, a northward prograding pattern of the limestones, away from the Aran anticline, can be observed (Fig. 11). The geometry of the erosional truncations and onlaps as well as the northward shelf edge progradation are coherent with a north-facing sedimentary slope related to coeval rising of the Aran anticline. The Ourlène limestone-marl intercalations merge westward in a single limestone body in continuity with the Urgonian limestones of the Sarrance anticline northern limb. Below this limestone, the Aran transverse fault zone juxtaposes the Sarrance Jurassic to lower Aptian succession with the Spicule marls covering the Aran Gargasian limestones (Fig. 7). Tens of meters-sized bodies of partially dolomitized limestone are intercalated in the Spicule marls along the fault system. We interpret this fault zone as a Clansayesian syn-sedimentary cross-fault that separated a more subsiding domain to the east from a less subsiding domain to the west. In this interpretation, the Gargasian limestones and overlying marls of the Aran anticline are stratigraphically equivalent to the lower part of the Sarrance Urgonian, while the Ourdinse limestone is the eastern extension of the upper part of the Sarrance Urgonian. Bed mapping shows that the Ourdinse limestone thins rapidly westward in the northern limb of the Sarrance anticline with possible lateral transitions to the Spicule marls (Fig. 7). This interpretation differs from previous works which assumed that the Ourlène limestones are thrust southward over the Spicule marls (Haller and Jardiné, 1986; Canérot et al., 1999). However, the existence of such thrust would implicate the existence of a lateral ramp separating the Ourlène and Sarrance Urgonian layers, while our mapping shows the continuity of the Urgonian between the two ridges. Hence, the limestone-marl intercalations at the eastern extremity of the Ourlène ridge are more logically interpreted as a northern equivalent of the similar intercalations south of the Aran anticline in the Bois de Gey-Pic Montagnon area discussed in the previous section.

North of the Sarrance anticline and Ourlène ridge, the Barescou succession forms a north-dipping monocline in the footwall of the Mail Arrouy thrust (cross-sections S1 to S3 in Fig. 4, and Fig. 7). The stratigraphic succession is more complete than in the Lourdios syncline, with the Clansayesian-lower Albian Spicule marls followed by the middle-upper Albian Black Flysch, itself subdivided into the Escot pelites and the Barescou sandstones (Roux, 1983; Souquet et al., 1985). The Barescou sandstones are an upper Albian (Vraconian) turbidite succession featuring up to m-thick beds of sandstone or/and conglomerate with cm-sized rounded clasts of Mesozoic carbonates and Paleozoic rocks (Roux, 1983). Bed thickness and grain size decrease westward, suggesting an eastern provenance. The steeply-dipping but variable dips in the Spicule marls and Black Flysch succession in the Aspe valley do not show an unequivocal growth folding pattern (cross-section S1 in Figure 4), but such a pattern may exist in the east where the dip of the Barescou sandstones is notably lower than that of the underlying Spicule marls and Escot pelites (croos-section S2 in Figure 4). The absence of equivalent coarse turbidites north of the Mail Arrouy thrust suggests that the Mail Arrouy already formed a ridge bounding the Barescou depocenter during the Albian.

4.1.5. The Lauriolle diapiric breccia

At the eastern end of the Ourdinse ridge, the Jurassic-Urgonian succession is replaced by the about 200 m thick Lauriolle breccia (Canérot and Lenoble, 1993; Cloix, 2017) (Figs. 7 and 10). On the western side, the carbonate succession shows in-situ brecciation increasing eastward and passing laterally to a polygenic breccia comprising mainly Jurassic elements in the lower part and Urgonian elements in the upper part (Cloix, 2017). Brecciation is posterior to the syn-metamorphic foliation of the limestones observed in the clasts. The presence of authigenic quartz crystals typical of the Keuper evaporites in the matrix of the polygenic breccia attests to diapirism. Canérot and Lenoble (1993) interpreted the breccia as resulting from diapir dissolution and collapse during the late Aptian, before being covered by the Albian marls. However, this would imply the unlikely hypothesis that carbonate metamorphism occurred at the sea floor. Alternatively, we postulate that, similarly to the other domains of the ZNP, metamorphism occurred during the Late Cretaceous favored by the blanketing effect of the flysch cover (Clerc et al., 2015, 2016), arguing for a later brecciation process.

4.1.6. Synthesis of salt tectonic evolution in the south-western CBB

The descriptions above indicate that the south-western CBB recorded a protracted salt tectonic activity during the Early Cretaceous. The first record of salt ridge rising would be the inferred absence of the Jurassic carbonates in the core of the Aran anticline, due to exposed diapir before the late Aptian. The same process may have occurred east of the Ossau valley at the Béon anticline (Fig. 2) which shows a welded structure of the Urgonian limestones similar to that of the Aran anticline.

In contrast to the Moncaut, Aran and Béon anticlines where it is limited to a narrow zone at the anticline crest, the Neocomian erosion and associated depositional hiatus increase southward across a km-wide zone in the south-western CBB, resulting in the deposition of the Urgonian limestones above the Dogger dolomite in the Layens-Ordinse ridge and the southern Tacha and Bergon klippes (Canérot et al., 1978) (cross-sections S2 and S3 in Fig. 4, and Fig. 7). Previous works ascribed this to uplift of faulted basement blocks in the Iberian mid-Cretaceous margin (Canérot et al., 1978; Puidefàbregas and Souquet, 1986; Combes et al., 1998). Although this interpretation is consistent with the geodynamic context, unequivocal evidence of contemporaneous salt wall rising at Moncaut, Aran and Béon anticlines, and the presence of Keuper facies underlying the whole area suggests that the rising of a wide salt inflation may have contributed to the uplift and erosion/non deposition of the carbonate succession in the southern domain of the CBB.

The rapid thickness variations of the Gargasian limestones in the Layens-Ourdinse overturned flap and at the crestal zone of the Sarrance ridge argue for rising of both diapiric structures during the late Aptian. Coeval rising of the Aran anticline is also shown by local pinching of the upper layers of the Gargasian limestone in the marls of the Lourdios syncline.

Halokinesis increased during the Clansayesian to early Albian with thick accumulations of Spicule marls in the Lourdios and Barescou synclines by salt withdrawal. The Lourdios syncline shows the typical pouch-like geometry of a minibasin subsiding between uprising adjacent diapirs, with marked growth strata on both limbs. Complex stratigraphy with limestone-marl intercalations, debris flow deposits and olistolites, erosional surfaces and onlaps attest important substratum mobility. The transverse Ponsuzon diapir and the transition between the Sarrance and Aran anticlines show the notable role played by transverse fault systems in partitioning the diapiric system. The latter transverse fault system probably made the transition between the eastern diapir where the Gargasian limestones deposited above the Keuper (Aran) from the less uplifted western domain where only the Upper Jurassic was eroded (Sarrance). Later, the uplift trend was inverted and the transverse fault system separated a more subsiding domain in the east (Aran, Ourlène) from a less subsiding western domain in the Sarrance northern limb. This inversion was probably favored by the previous larger rise of the salt in the east.

However, salt tectonics during the Clansayesian to early Albian often implied moderate bed uprising. Indeed, the uppermost beds of the Lourdios and Barescou minibasins are also folded and thrust (Sections 1 to 3 in Fig. 4, and Figs. 7, 8, 9 and 10). We interpret this as the result of later salt-wall squeezing, traduced in the present structure by diapir welding, megaflap overturning and salt extrusion. The Lauriolle breccia may also be related to diapir squeezing, posterior to the Late Cretaceous metamorphism in this case. However, dating the late diapir squeezing is difficult due to erosion of post-Albian strata. This dating is discussed below in the frame of a general geodynamic model for the CBB evolution.

4.2. The Tres Crouts structure: a polygonal multi-stage salt structure

Located in the eastern part of the CBB, the Tres Crouts structure corresponds to a polygonal weld resulting from the interference of E-W to ESE-WNW (the general trend of the CBB) and NNE-SSW trends (Figs. 2 and 12). The latter corresponds to the transverse trend which characterizes the eastern termination of the CBB at its transition to the Ossun basin (Fig. 2). The map presented in Figure 12 is based on the BRGM geological map (Casteras et al., 1970a) and includes structural data from Lanusse (1969), new stratigraphic and structural interpretation at the NE border of the Tres Crouts structure from Cloix (2017), and precision of contours and new structural data along cross-section S4 (Fig. 4) from the present work. In the western part of the structure, where the weld outcrops at the level of the Lower Liassic breccias, there remain lenses of Keuper facies, ophite bodies and Paleozoic metasediments (Figs. 12 and 13). A remarkable feature is the centripetal vergence of the structure, i.e. the inner compartment features an overturned flap with an ellipsoidal syncline axial trace, resulting in two recumbent synclines with opposite vergence in profile (cross-section S4 in Fig. 4).

In the northern area, the occurrence of the subvertical Dogger dolomite against the northern flank of the weld surface may result from the direct deposition of the dolomite above the Keuper in a Jurassic diapir, but alternatively it may result from the tearing of the Lias off the diapir margin during salt flow. Whatever the case, the dolomite layer against the welded surface features pervasive brecciation cemented by dolomite and subsidiary quartz (Cloix, 2017) interpreted as resulting from the diapir squeezing process. In the inner syncline, the Kimmeridgian is thinner in the reverse flap than in the normal limb, suggesting a growth folding geometry, and thus a possible diapiric activity during the Jurassic with accumulation of the Kimmeridgian in the enclosed minibasin. Cross-section S4 in Figure 4 tentatively shows continuation of growth folding up to the Albian Black Flysch.

In the north-western part of the Tres Crouts structure, the outer flank shows a truncation surface cutting eastward the Neocomian and Upper Jurassic down to the Dogger dolomite and overlain by the upper Aptian Urgonian limestones (Fig. 12). This surface is identified as a fault on the BRGM geological map (Casteras et al., 1970a), but from its geometry and location above the weld we consider that it more likely represents a Neocomian erosional surface analog to the one at Moncaut (Fig. 6). In the north-eastern part, the Black

Flysch lies on another erosional surface that truncates the northern flank of the weld eastward from the Urgonian limestones down to the Dogger dolomite, thus merging with the Neocomian erosional surface (Fig. 12). East of a N-S trending transverse fault, the flysch is in contact with the Liassic carbonates of the southern flank. Owing to the divergent polarity of bedding, we interpret this contact as the eastern extension of the weld. More to the east, the northern and southern welds merge in a north-vergent thrust weld extending eastward to the CBB extremity (Fig. 2). Above the erosional surface and against the eastern part of the northern weld, the Black Flysch comprises at its base local intercalation of conglomerate reworking the underlying carbonates with up to tens of cm-sized clasts. The conglomerate is not as continuous as shown on the BRGM map (Casteras et al., 1970a) and shows variable clast composition: it comprises mainly Urgonian limestone clasts and rare small Dogger dolomite clasts where it rests above the Urgonian limestones, and mainly Jurassic clasts with subordinate Urgonian clasts against the weld, demonstrating a local origin and short transport (Cloix, 2017).

Hence, the Tres Crouts structure results from a multi-stage evolution. Salt diapirism likely begun during the Jurassic, with the Dogger dolomite depositing above a piercing salt wall in the NE, and the Kimmeridgian accumulating in a minibasin enclosed in the polygonal diapiric structure. The erosional surfaces record continuing salt rise during the Neocomian and the late Aptian-Albian. Later deformation resulted in further fold tightening, welding and local weld reactivation as a thrust. Jurassic diapirism in the CBB is not described in previous works which consider that the Jurassic tectonics was controlled by N-S trending faulted blocks while diapirism begun in Early Cretaceous times with development of E-W trending faults (James and Canérot, 1999; Canérot et al., 2005). A few km south-east of Tres Crouts, submarine slides in the Kimmeridgian of the Pibeste ridge (James et al., 1996) attest to tectonic activity in the eastern CBB at that time, and the structure of the Tres Crouts Kimmeridgian suggests that this activity may involve salt wall rising. The Saint-Pé de Bigorre ridge, located close to the north of the Tres Crouts structure, is an E-W trending squeezed diapir (cross-section S4 in Fig. 4, and Fig. 12) with a complete Jurassic-Lower Cretaceous succession but with all stratigraphic intervals featuring a reduced thickness, also suggesting continuous salt wall rise throughout the Jurassic and Early Cretaceous.

The Tres Crouts metamorphic zone occurs in the central minibasin where it affects the Kimmeridgian limestones in an area about 2 X 1 km (Fig. 12), characterized by marbles with scapolite crystals (replaced by calcite, quartz, chlorite and white mica) (Casteras et al., 1970a; Villard, 2016). In this zone, Raman spectroscopy of carbonaceous material yielded peak paleo-temperatures up to 470-490°C (Villard, 2016; Ducoux, 2017). The borders of the high temperature zone are narrow (200-400 m) with very high thermal gradient, up to 30°C/100 m (Villard, 2016), passing in the rest of the Tres Crouts structure to temperatures about 340-370°C analogous to the most common temperatures recorded elsewhere in the CBB (Menant et al., 2016; Corre, 2017). The structural location of the metamorphic zone and its very high lateral gradient of temperature attest to a thermal anomaly probably related to fluid flow in the diapiric structure. The thermal event is not dated but it ought to be relatively late in the salt tectonic history as the Pyrenean Cretaceous metamorphism was related to the blanketing effect of the Upper Cretaceous flysch (Clerc et al., 2015).

4.3. The Pyrenean inversion: The North-Pyrenean Frontal Thrust and the Licq fault

4.3.1. The North-Pyrenean Frontal Thrust

At the eastern end of the CBB, the NPFT is marked by the Ossun diapir (Fig. 2), a salt ridge formed during the Mesozoic extension and reactivated and squeezed during the Pyrenean inversion -but still up to 800 m wide- (Casteras et al., 1970a; Canérot et al., 2005). Westward, the diapir passes laterally to a thrust that juxtaposes the limbs of two synclines, with the Black Flysch of the Forêt de Mourle syncline in the hanging wall and the Cenomanian flysch in the reverse limb of the footwall syncline (Fig. 2 and cross-section S4 in Fig. 4). There is no exposure of Keuper facies along the thrust, but lenses of Keuper anhydrite have been drilled between 85 and 154 m depth in the St-Vincent well (see Supplementary Data, Fig. S1). The juxtaposition of two syncline limbs as well as the occurrence of Keuper lenses strongly suggests that the NPFT emerging between the Ossun diapir and the Rébénacq transverse diapiric structure (Fig. 2) corresponds to a former salt wall that extended all along the eastern part of the CBB and was squeezed and welded during the Pyrenean compression. The erosional truncations at the base of the Upper Cretaceous and base of the Lower Cretaceous north of the Grand Rieu High (cross-section S4 in Fig. 4, and Supplementary Data, Fig. S2) result from uplifting of the northern flank of the diapir during the extensional period, similarly to the model of Canérot et al. (2005) for the Ossun diapir a few km to the east of our cross-section. The km-scale progressive unconformity that involves the Campanian-Maastrichtian flysch and overlying Neogene strata in the thrust footwall suggests that diapir squeezing was activated from the beginning of the Pyrenean convergence and that the thrust front remained localized on the same structure until the Tertiary, without noticeable northward propagation. The lenses of Paleozoic rocks existing at the hanging wall of the emerging thrust are interpreted as short-cuts of faulted blocks of the southern edge of the Grand-Rieu High.

By analogy with the eastern segment, the blind segment of the NPFT thrust west of the Rébénacq transverse diapiric structure can also be interpreted as a welded salt wall.

This salt wall may have been the feeder of the Lasseube diapir, a 10 km-long salt sheet enclosed in the lower Eocene a few km east of cross-section S1 in Figure 4 (Fig. 2). We show in cross-section 1 a diapir in the subsurface in a position equivalent to that of the Lasseube diapir, as well as hypothetic Keuper facies lens pinched along the NPFT. Similarly to the eastern segment, the western NPFT remained active during most of the Pyrenean convergence and only a limited displacement (about 1 km) was transferred more to the north in the Pau anticline during the Eocene.

4.3.2. The Licq fault

At the south-western border of the CBB, the Licq fault juxtaposes the Keuper facies of the Layens-Ourdinse salt wall with the Albian Mendibelza conglomerates of the Flysch Noir Group on the southern side (cross-section S1 in Fig. 4). The fault dips steeply southwards and the Layens succession appears as an overturned footwall flat, with the Keuper layer a few tens of meters thick. The Licq fault extends along tens of km westward at the southern border of the Mauléon basin with the same geometry and the Mendibelza conglomerates exhibit there southward dips and a ramp against the fault represented above the topographic surface in cross-section S1. The apparent footwall flat in the Keuper level, as well as the occurrence of several diapiric structures adjacent to the Licq fault in the southern Mauléon basin lead to consider the fault as a squeezed salt wall with a corresponding flap in its northern flank (James and Canérot, 1999; Teixell et al., 2016; García-Senz et al., 2019). Similarly to the NPFT, this interpretation will be discussed in the frame of the geodynamic model presented below.

5. Discussion: Hyperextended rift geodynamics and salt tectonic evolution

In this section, we integrate the CBB salt structures described in the previous sections in a basin-scale model of hyper-extended Cretaceous rifting and inversion by the Pyrenean orogeny. The model is illustrated in Figure 14, based on the sequential restoration of the balanced cross-section S1 in Figure 4.

5.1. Geological basis for basin-scale restoration

The sequential restoration in Figure 14 is based on the following essential geological features and inferences deduced from them.

1) The CBB Mesozoic cover behaved as a continuous lid, pierced by diapirs with openings not exceeding a few km wide. In the western CBB, our mapping shows the structural continuity across the Lourdios syncline, and the observed lateral terminations of the Sarrance anticline suggest a limited width of the diapir opening at the origin of the salt extrusion. The lack of exposure precludes determining opening of the former Mail Arrouy diapir, but the lateral termination of the Mail Arrouy thrust east of the Ossau valley (in the Moncaut anticline; Figs. 2 and 6) also suggests a limited opening. The map structure of the eastern CBB shows continuity across the whole belt with lateral termination of diapirs (Moncaut, Tres Crouts; Figs. 2, 6 and 12).

2) As demonstrated by the structural location of most of the lherzolite bodies (Figs. 2, 4 and 7), the Mesozoic cover lid was detached on the Triassic evaporite layer and its central part rested directly on an exhumed mantle tract (Jammes et al., 2009; Lagabrielle et al., 2010, 2019a and b; Tugend et al., 2014; Teixell et al., 2016).

These features imply that the basement of the ancient continental margins had a smooth-slope topography allowing for continuous cover décollement, i.e. steeply-dipping normal faults were absent or had limited offsets not interrupting the continuity of the Triassic décollement layer. Cover gliding also implies denudation in the proximal part of the margins.

3) The uppermost part of the margins could be affected by basement faults. To the south, restoration of the Lakora thrust structure and the stratigraphy of the Mendibelza and overlying Upper Cretaceous conglomerates and breccias observed to the west in the neighbouring Mauléon basin argue for deposition against a basement fault scarp that bounded the Iberian shelf domain (future Axial Zone) submitted to erosion (Durand-Wackenheim et al., 1981; Boirie and Souquet, 1982). North of the fault scarp, the onlap surface of the Mendibelza conglomerates corresponds to the basement top of the proximal margin (i.e. necking zone) tilted to the north (i.e. basinward). Hence, this surface can be interpreted as the denuded Triassic gliding surface along which the cover lid slid northward (Teixell et al., 2016; Saspiturry et al., 2019). Following Teixell (1993), we infer that the future Bedous Triassic unit was preserved from erosion or gliding in a fault block existing to the south. To the north, the proximal European margin and shelf correspond to the Grand-Rieu horst (Fig. 4)

4) Although a precise restoration of the basin dimensions is difficult, approximate indirect estimations can be made. The footwall of the NPFT corresponds to the European margin (Teixell et al., 2016, 2018), suggesting a width of around 38 km for the latter. Uncertainty is greater for restoring the Iberian margin basement, as it is presently the substratum of the CBB whose internal structure and hence the amount of Pyrenean shortening, remain unknown. In the lack of data, we assume a relative symmetry with respect to the European margin, being aware that this uncertainty impacts the estimation of the width of the denuded upper margin and ultimately of the total Pyrenean shortening (see below Section 5.3.4). Based on the location of the Sarrance and Mail Arrouy lherzolites, a minimum

width of 17 km is inferred for the exhumed mantle domain (Teixell et al., 2016). Using this value implies that the cover lid glided from both margins, with the southern CBB (Layens) resting on the distal Iberian margin and the northern CBB (Oloron) resting on the European distal margin, with a wide denudation of both upper margins.

5.2. Rift basement structure

Different models of crustal deformation have been proposed for the Cretaceous rifting in the CBB domain and neighbouring Mauléon basin. Teixell et al. (2016) and Asti et al. (2019) adapted to the CBB the model of ductile crustal extension first proposed by Clerc and Lagabrielle (2014) and Clerc et al. (2016) for the eastern and central Pyrenees, and recently generalized as a “smooth-slopes basin” model to various peri-Iberian Cretaceous rifts by Lagabrielle et al. (2020). Teixell et al. (2016) restoration provides a basement top geometry which satisfies the basic geological features listed above.

Masini et al. (2014) proposed for the Mauléon basin an alternative model inferring a north-dipping intracrustal detachment emerging to the south in normal faults bounding tilted basement blocks (Jara-Arbailles and Mendibelza). Gomez-Romeu et al. (2019) recently transposed this interpretation in an isostatically compensated kinematic modelling of the CBB transverse. Similarly to the Teixell et al. (2016) interpretation, their model shows continuity of the CBB Mesozoic lid and its gliding from the European margin on a 19 km wide exhumed mantle domain, associated to a wide denudation of the upper margin. However, the model also implies tilted basement blocks with attached Jurassic cover south of the CBB which do not conform with the thin geometry of the Paleozoic in the Iguntze and Bedous-Laruns thrust units, as well as with the northward tilting of the basement top in the former unit.

Saspiturry et al. (2019) give a new interpretation of the Mauléon basin which accounts for the structure of the Iberian proximal margin, via a south-dipping intra-crustal detachment causing the northward tilting of the Mendibelza onlap surface in Albian times, then a new northward detachment explaining the southward-tilting of the Arbailles block during the Late Cretaceous. However, such a flip-flop evolution remains hypothetical and the model does not show denudation of the European margin.

Discussing further a crustal-scale model of rifting is out of the scope of this paper. The evolutionary model used here uses a basement top geometry analogous to that of Teixell et al. (2016), adapted to the observed geological features of the CBB. It does not intend to preclude any alternative mechanism of crustal deformation as long as the basic geological constraints are satisfied.

5.3. Salt tectonics and basin evolution

5.3.1. Late Triassic to Aptian extension

The Jurassic to Aptian corresponds to a period of low subsidence with accumulation of ca. 1.5 km thick platform carbonates above the salt-bearing Triassic unit (Fig. 14, stage 1). The original thickness of the latter is unknown due to high salt mobility and probable salt dissolution at exposed diapirs (James and Canérot, 1999; Canérot et al., 2005), but the observed development of salt tectonics and large Keuper volumes remaining in the present profiles argue for a thickness of several thousands of meters. It must also be noted that, although the top Triassic Keuper facies is commonly reported as the main salt detachment or diapiric unit in the Pyrenees, the occasional, but frequent existence of Middle Triassic Muschelkalk limestones in the Chaînons Béarnais ridges and other Pyrenean diapirs (e.g. Canérot et al., 2005; Ortí et al. 2017) suggests that the basal detachment level must stratigraphically underlie the limestones. Canérot et al. (2005) proposed that it may correspond to a shale level. Alternatively, it may correspond to sub-limestone evaporites such as those reported from the subsurface of the Ebro basin (“middle Muschelkalk” evaporites, including halite; Jurado, 1990). Hence, it is likely that the highly disrupted Muschelkalk carbonate lenses in the Chaînons Béarnais were originally interbedded in shale/evaporite deposits, and hence the décollement layer illustrated in our restoration is not restricted to the Upper Triassic Keuper but also includes the Middle Triassic. In our restoration, an original thickness of the Middle-Upper Triassic about 3000 m is deduced from balancing constraints. This is consistent with the fact that the NPZ corresponds to a branch of the peri-Iberian Triassic rift system which concentrated thick evaporite deposition (Soto et al., 2017; Lagabrielle et al., 2020, and references therein). Curnelle (1983) reported up to 900 m of salt-bearing facies in little deformed areas of the Aquitaine basin north of the CBB, while Espurt et al. (2019) show an interpreted seismic profile with up to about 3000 m of Middle-Upper Triassic on an undeformed tilted block of the south-central Aquitaine basin.

Some authors contemplate incipient rise of salt anticlines during the Jurassic in the Aquitaine Basin (Mediavilla and Mauriaud, 1987; Serrano et al., 2006). We consider likely that basement faulting triggered salt movements in the thick Triassic layer of the CBB during this time, because as discussed above, the Tres Crouts and Saint-Pé-de-Bigore salt structures suggest initial salt mobility during the Jurassic. Hence, our cross-sections in Figure 4 and restoration in Figure 14 assume a slight thickness increase of the Jurassic in salt synclines. Diapir rising is more evident during the Neocomian period, with erosion of the Jurassic and depositional hiatus of the Neocomian on uplifted areas that can be narrow salt wall crests (Moncaut, Aran and Béon anticlines) or a wider salt massif in the southern CBB. At least part of the Neocomian salt walls of the CBB pierced to the surface and were overlapped by Aptian deposits (Asasp, Aran, Béon), similarly to many coeval diapirs in the Aquitaine Basin (Mediavilla and Mauriaud, 1987; Canérot et al., 2005; Serrano et al., 2006). Salt wall rising and minibasin subsidence accelerated during the latest Aptian (Clansayesian), contemporaneously to the drowning of earlier carbonate platforms and the individualization of deeper depocenters. This is marked by the onset of the Spicule marls deposition, probably traducing acceleration of basement stretching and crustal thinning. Carbonate sedimentation persisted on the rising diapir crests until their definitive drowning in the earliest Albian (Fig. 14, stage 1).

5.3.2. Albian climactic rifting

The Albian-early Cenomanian period is considered as the main rifting period in the NPZ, marked by the deposition of the upper part of the Spicule marls followed from the late early Albian by the thick sequences of the Black Flysch Group (Souquet et al., 1985; Debroas, 1987, 1990). Both hyper-extended continental margins with smooth basement top were formed and the mantle was exhumed in between (Fig. 14, stage 2). Down-margin gliding of the cover succession resulted in the denudation of the upper margins and separation of the diapirs from the basement faults on which they initiated. Eventually, they were placed on top of the exhumed mantle where the Triassic salt detachment collected the peridotite blocks.

On the Iberian side, the sedimentary cover of the southern shelf (the future Axial Zone) was eroded, and incision down to the Paleozoic fed the Mendibelza conglomerates in alluvial fans onlapping up-margin the basinward tilted and denuded basement top (Boirie and Souquet, 1982; Teixell, 1993; Saspiturry et al., 2019). South of the Mendibelza conglomerates, in the Iberian shelf, we show the above-mentioned faulted block with preserved Keuper that will become the Bedous Triassic thrust unit during the Pyrenean inversion (Teixell, 1993) (cross-section S1 in Fig. 4). As an alternative, García-Senz et al. (2019) interpreted the Bedous Triassic unit as a salt sheet expulsed from the base of the Mendibelza conglomerates, resulting in an hypothetic weld at the base of the conglomerate that we consider unlikely in the absence of any remain of Keuper facies, Muschelkalk or ophite bodies which otherwise are common in the Bedous unit as well as along the CBB welds (Fig. 13). No conglomerates equivalent to the Mendibelza are known along cross-section S1 on the European side and we postulate that the basement of the Grand Rieu High was not largely exposed to erosion, as was the Axial Zone. This does not exclude local exposure at some places, as it is suggested by a conglomerate reworking Paleozoic clasts at the base of the Black Flysch in the northern limb of the Forêt de Mourle syncline (Fig. 2).

Our field observations show that folding related to diapir rising and minibasin subsidence by salt withdrawal was very active during deposition of the Spicule marls and Black Flysch. Restoration indicates that the Barescou depocenter corresponds to the axis of the Albian basin, with the maximum thickness (up to ca. 3500 m) of Spicule marls and Black Flysch, culminating with the Barescou turbidites. This location of the basin axis was already proposed in the frame of a former continental rift model (e.g. Canérot et al., 1978; Combes et al., 1998). Here, it is consistent with the inferred position and width of the exhumed mantle domain discussed above.

The lower Cenomanian unconformity which marks the end of the maximum rifting stage in the NPZ is observed in the present section on the northern limb of the Asasp diapir and on the future Axial Zone, as well as, to the north, on the northern Grand-Rieu High and in the Arzacq-Tarbes basin (Canérot et al., 2005; Serrano et al., 2006; see also cross-section S4 in Fig. 4). While erosion in the south and north may be ascribed to an uplift of the rift shoulders, erosion in the deep basin is more difficult to interpret. It may traduce rising of the diapirs at the lower margin, but we see unlikely that it was related to a terrestrial emersion because the erosion surface is observed between two deep-water flysch units.

5.3.3. Cenomanian to Santonian extension

Stage 3 in Figure 14 portrays the end of the Pyrenean rifting, before the onset of the Pyrenean inversion by late Santonian times. The calcareous Upper Cretaceous flysch units accumulated in the basin while carbonate platforms grew on the rift shoulders (the future Axial Zone and, north of our section, the Arzacq Basin, Biteau et al., 2006; Serano et al., 2006). The geodynamic context of the North-Pyrenean basin during the Cenomanian to Santonian period has been interpreted in different ways, either as transpressive, or continued extensional, or simply in post-rift subsidence (see discussion and references in Clerc et al., 2016, and Vacherat et al., 2016). Clerc et al. (2016) suggest from their study in the eastern NPZ that extension may have continued during this period, explaining post-metamorphic exhumation of the Mesozoic carbonates along the extensional detachments and conglomerate accumulation along some fault escarpments. This assumption is supported in the Mauléon basin by the conglomerate bodies that are deposited above the Mendibelza conglomerates up to the Santonian Ibarrondoa breccia, recording continued erosion of the Paleozoic of the future Axial Zone and its Upper Cretaceous platform limestone cover (Casteras and Souquet, 1970; Durand-Wackenheim et al., 1981; Teixell, 1993). Saspiturry et al. (2019) also interpret the stratigraphic organization of the Mauléon basin as indicative of continuous extension during the Late Cretaceous, with the formation of a new north-dipping intracrustal detachment and the lower Cenomanian unconformity as a consequence. Hence, our restoration shows a few km increase of mantle exhumation and margin extension compared to the previous stage. It also shows further sliding of the detached cover, resulting in increased width of the denuded domains at upper margins. Due to near welding at the base of the Barescou depocenter, the maximum thicknesses of Cenomanian to Santonian flysch units are accumulated laterally above the distal parts of the continental margins in association with withdrawal of the underlying Keuper and its extraction in open diapirs.

5.3.4. Pyrenean inversion

Stage 4 in Figure 14 shows an intermediate stage of positive inversion of the North-Pyrenean basin at the end of the Cretaceous. Since the onset of convergence, the exhumed mantle has been subducted and the toe of the Iberian margin has begun to overthrust the European margin, initiating the NPFT. This stage corresponds to the proto-collision of Teixell et al. (2016), during which the crust recovered its original thickness before the full collisional overthickening at Eocene times. Due to basement shortening, the detached cover behaves as a thin-skinned pop-up structure climbing on both margins. Shortening of this sedimentary lid is achieved by fold tightening and diapir squeezing, mostly by contraction of the large diapiric zones of the denuded upper margins. Flexural foreland basins begin to form with the Upper Cretaceous flysch series onlapping both upper margins. The still reduced crustal thickness and continued thermal subsidence (Angrand et al., 2018) maintained most of the deformed belt in submarine conditions, but we cannot rule out the existence of local emerged reliefs as the one tentatively shown in the restoration resulting from contraction of the Licq diapir. On the European margin, the deposition of the Upper Cretaceous flysch concomitant to diapir squeezing resulted in the growth strata fan observed in the NPFT footwall. The flysch laps on the Paleozoic basement or Triassic on the southern part of the Grand-Rieu High and, more to the north, on an erosional surface which cuts the pre-

Campanian succession (see Fig. 9 in Canérot et al., 2005) and fed the basal breccia of the flysch. We suggest that the tilt of the onlap surface may not be due to flexural subsidence alone, but also to the salt withdrawal and resulting welding of the cover above the Grand-Rieu High induced by the flysch accumulation, similarly to the scenario proposed by Canérot et al. (2005) for the eastern extremity of the CBB on the Ossun section (Fig. 2).

Stage 5 in Figure 14 is the present structure after completion of the Pyrenean collision from late Eocene to earliest Miocene times. Squeezing of the diapiric zone of the upper European margin resulted in its welding to become the present NPFT, which remained active at least until the mid-Eocene. We interpret that diapir squeezing fed the Lasseube diapir forming a salt sheet covered by the basal Eocene strata. At the beginning of the Eocene, propagation of the cover décollement (possibly favored by welding of the NPFT at that time) resulted in the formation of the Pau anticline a few km northward (see cross-sections in Canérot et al., 2005, Lagabrielle et al., 2010, and Teixell et al., 2016). On the Iberian side, the Licq diapir was welded to form the present steeply-dipping fault between the Mendibelza conglomerates and the Black Flysch turbidites, explaining the strong facies contrast between the two formations now juxtaposed by the fault. Then, southward propagation of the CBB décollement detached the Mendibelza conglomerates and a slice of its Paleozoic substratum, the latter probably corresponding to the short-cut of the footwall of a former normal fault, thus initiating the Lakora-Larra thrust system which propagated into the northern Jaca basin and remained active until the Bartonian (Teixell, 1996; Labaume et al., 2016; Labaume and Teixell, 2018). Contrary to the NPFT where tectonic activity remained localized during the whole Pyrenean orogeny, the full collision of the European and Iberian margins during the Late Eocene-Oligocene resulted in the development of the basement thrust imbricate of the Axial Zone which uplifted and deactivated the Lakora-Larra thrust system (Teixell et al., 2016, 2018). The whole CBB was tilted northward above the back-limb of the Axial Zone culmination, in the hanging wall of the NPFT.

The restoration in Figure 14 implies 101 km of total Pyrenean shortening, corresponding to 75 km shortening in the North-Pyrenean wedge (including 17 km of subduction of exhumed mantle, and 1 km shortening on the Pau anticline north of the restored section) and 26 km shortening in the Axial Zone basement (Gavarnie, Broto and Guarga thrusts; Teixell, 1996; Teixell et al., 2016; Labaume and Teixell, 2018). Although these values suffer uncertainties resulting from those on the length of the pre-orogenic margins as discussed above, they are close to those deduced from kinematic modelling by Gomez-Romeu et al. (2019), and coherent with results of Espurt et al. (2019) who calculated 127 km shortening on the Nestes-Ainsa cross-section 80 km to the east, including about 12 km shortening in the Aquitaine basin north of the NPFT that is not comprised in our restoration of the CBB-Jaca cross-section. It is interesting to note that the latter implies less Axial Zone shortening than the Nestes-Ainsa section where the Iberian crustal prism is more developed, but more shortening in the northern Pyrenees. This is consistent with the fact that the Pyrenean rift was wider westward, i.e. toward the oceanic domain of the Biscay Bay, thus influencing lateral changes in the distribution of the shortening for similar values of total convergence, and explaining the more recent exhumation of the NPZ and emersion of the Pyrenean relief in the west (Vacherat et al., 2014; Bosch et al., 2016; Labaume et al., 2016; Teixell et al., 2016).

5.4. Driving mechanisms of salt walls rising

Restoration of the CBB structures shows a protracted history of salt ridge rising, probably beginning in the Jurassic and continuing throughout the rifting and subsequent Pyrenean inversion episodes. If the initial stages up to the Aptian can be interpreted as diapirs formed above basement normal faults (Canérot, 1988, 1989), conditions of loading changed when the diapirs were detached from their original basement during the mid-Cretaceous downslope gliding.

A first consequence of the cover gliding is the denudation of the proximal margins, allowing for deposition of the Mendibelza conglomerates on the denuded basement top and Permo-Triassic sandstone tegument (Teixell et al., 2016; Saspiturry et al., 2019). We also assume that evacuation of Keuper facies under subsiding minibasins at the rift center together with extension resulted up margins in wide diapiric zones devoid of carbonate cover. To the south, such inflated zone may have separated the proximal domain of Mendibelza conglomerates from the more distal domain of flysch. Using the margin lengths discussed above, assuming that diapirs did not exceed 2-3 km width in the basin center, and length-balancing the known cover elements (Mendibelza conglomerates and CBB carbonates), we deduce a 14 km wide diapiric zone between the Mendibelza conglomerates and Layens ridge on the Iberian margin, and a 25 km wide diapir on the conjugate upper European margin. Comparable wide diapirs resulting from gravity sliding-induced denudation and/or extension have been inferred recently on the Brasilian passive margin (the “Albian Gap”; Jackson et al., 2015; Pichel et al., 2019).

Furthermore, we infer that gliding of the cover lid down the margins most probably implied not only tectonic denudation of the proximal margins, but also shortening at the conjugate margin toes and over the central exhumed mantle where the slid mass accumulated. Jammes et al. (2010) discussed interactions between salt tectonics and extensional detachment systems in the Bay of Biscay and western Pyrenees. They conceptually oppose margins with post-rift salt where the deformation of the detached cover is purely gravitational, implying that contraction at the toe of the gliding cover compensates extension at the upper part (e.g. Brun and Fort, 2011), to margins with pre-rift salt layers as the Pyrenees where the salt decouples extensional deformation between the basement and cover. In the latter case, Jammes et al. (2010) argue that the cover may only feature extensional rafts because the basement and cover are extended coevally (and the salt in between is stretched), so the whole system is extended and does not need contraction. Although the Ibis anticline in the center of the Parentis basin (reported in Bois et al., 1997, and Masse, 1997) may have been related to gravitational contraction at Albian times, Jammes et al. (2010) consider that the extensional structures of the basin are not linked with compressional structures of the same age. Conversely, we consider that an important effect of gravity cannot be excluded in the slopes of actively stretching margins containing a pre-rift salt unit as the Pyrenees. If the continuity of the salt layer is not broken, the gravitational displacement can exceed tectonic stretching and hence contraction being caused by crowding at the basin axis coeval with extensional denudation upslope. In the case of the CBB, we emphasize that the salt ridge rising and folding restored at stages 2 and 3 in Figure 14 would be analogous to the fold and thrust system characterizing compressional diapirs at lower continental margins (Rowan et al., 2004; Brun and Fort, 2011; Jackson and Hudec, 2017). Figure 15 illustrates the close resemblance between the Sarrance anticline and adjacent Lourdios syncline, as well as the Tres Crouts structure (cross-sections S1 and S4 in Fig. 4), with compressional diapirs and adjacent pouch-like minibasins observed in the lower continental margin of Angola and obtained by analogical modelling (Brun and Fort, 2004).

We indicate that some recent works propose that the contact of the lherzolite and associated Paleozoic bodies with the overlying carbonates represent the original detachment contact between the exhumed mantle and the Mesozoic cover, inferring that the CBB anticlines correspond to late structures formed during the Pyrenean inversion (Lagabrielle at al., 2010, 2019a and b; Corre et al., 2016; Corre, 2017). This interpretation conflicts with the evidence that the CBB anticlines begun growing at least from the earliest Cretaceous, well before mantle exhumation during the Albian. Although we agree that the lherzolite bodies were teared off the mantle along the detachment system described by the above-cited works, we believe more probable that the bodies outcropping at the upper part of anticlines (Sarrance, Moncaut, St-Pé-de-Bigorre) were dynamically pushed up 4-5 km to their present position by the salt ascent in the salt walls, similarly to peridotite bodies of equivalent size in the Sivas diapiric province (Kergaravat et al., 2017). The latter case corresponds to a foreland context where compression squeezed the diapirs and probably favored the uprise of dense bodies. In the CBB case, our view suggests that contraction may have acted not only during the Pyrenean compression but also earlier in the rifting context. As the Urdach lherzolite shows evidence of being exposed to the sea floor in late Albian times (Fortané et al., 1986; Jammes et al., 2009; Debroas et al., 2010; Lagabrielle at al., 2010, 2019 b; Corre, 2017), we place the Saraillé lherzolite high in the Sarrance salt wall in the Albian restoration of Figure 14.

6. Conclusions

The revisit of the Chaînons Béarnais salt structures presented in this paper and summarized in four new cross-sections and detailed mapping of key-areas emphasizes their relevance in the architecture and geodynamic evolution of the North-Pyrenean basin and subsequent thrust wedge. Our work shows that the fold-thrust structure of the Jurassic-Cretaceous sedimentary cover corresponds to salt-walls and minibasins detached and squeezed above a thick Middle-Upper Triassic evaporite-rich layer (here collectively referred to as Keuper facies). A long history of salt migration is responsible for the numerous sedimentary discontinuities of diverse ages reported in this segment of the Northern Pyrenees, and can be summarized as follows:

1) Salt-walls most probably began to rise above basement normal faults during the early stages of Mesozoic extension. Following early salt movements during the Jurassic, erosions and hiatus mark the rising during the Neocomian of narrow pierced salt walls in the basin axis and a wider salt inflation in the southern basin margin.

2) From the latest Aptian, the onset of margin hyperextension resulted in the acceleration of salt wall rise and minibasin subsidence with limestone shelves on ridge crests prograding toward deeper minibasins dominated by thick marl deposition. During the Albian, the main rifting stage in the North-Pyrenean basin, the limestone shelves were ultimately drowned, and the whole CBB cover glided down-margin in the domain of deep flysch sedimentation as the continental margins were pulled apart. The diapiric structures were disconnected from parent basement faults and the axial part of the cover lid was put on top of exhumed mantle, as indicated by lherzolite slices embedded in the Triassic Keuper.

Meanwhile, the proximal margins were denuded, and, in the case of the southern shoulder, submitted to erosion that fed conglomerate sedimentation on the denuded proximal margin. Our margin restoration suggests that 15-25 km-wide diapiric zones may have occupied the denuded margins between the domain of conglomerate sedimentation and the slid CBB cover lid, analogous to the early Cretaceous denudation inferred in the modern Brazilian continental margin.

3) Conglomerate sedimentation in the proximal Iberian margin suggests persistence of extension during the Cenomanian to Santonian. Our restoration suggests that the flysch accumulated during that period in the deep basin was thicker above the distal margins, due to withdrawal of previously inflated salt, than at the basin axis, where it was limited by primary welding of the central minibasin system on the exhumed mantle.

4) From the onset of Pyrenean convergence in the late Santonian, the exhumed mantle was subducted and the Iberian margin was thrust above the European margin. The detached sedimentary lid then behaved as a pop-up structure climbing up-margins while the large diapiric zones of the denuded upper margins and the central salt walls were contracted and squeezed.

Part of the salt-related folding before the Pyrenean orogeny could have been caused by gravity-driven contraction. The syn-sedimentary salt structures of the Mesozoic CBB show typical features of deep water contractional salt systems such as pouch-like minibasins, salt-wall welding, salt overhangs, and salt extrusions. The context of cover gliding during the Mesozoic extension suggests that the salt structures were affected by contraction at margin bottoms and above the exhumed mantle coeval with extension upslope, in analogy to what occurs on the gravity-dominated, Angola-type modern distal margins. However, at variance with those modern margins, the North-Pyrenean slid unit was detached above a pre-rift salt layer and formed a continuous lid between the two margins and the central basin, and probably part of the contraction was caused by crowding at the basin axis. This implies that part of the salt squeezing may have been achieved in the rifting stage and the Pyrenean inversion was only responsible for final shortening and northward tilting of the whole structure in the hanging wall of the NPZ.

The salt tectonic style here described for the CBB is linked to the smooth topography of the continental margin slopes where the continuity of the décollement layer was not offset by major rift or thrust faults to prevent generalized décollement during the two tectonic phases. This shortening-by-gravity model was never applied to the Mesozoic Pyrenean basins and may find application in other segments of the belt and of the peri-Iberian basins (e.g. Parentis). The model involves formation of wide denuded domains up-margins, a concept that may be applied to other margins where gravity gliding on salt décollement layers is a major mechanism.

Acknowledgments

This work was supported by the French National Research Agency PYRAMID project, the BRGM-RGF (Bureau des Ressources Géologiques et Minières-Référentiel Géologique de la France) Pyrénées program, and the spanish MINECO/MCIU projects CGL2014-54180 and PGC2018-093903-B-C21. The BRGM is acknowledged for providing a seismic profile, Midland Valley (now Petroleum Exploration) for providing academic licenses of the Move software for structural modelling, and Seismic Micro-Technology for providing the Kingdom software used for seismic interpretation. We thank A. Gay, C. Poitevin and S. Minici for management and help in interpretation of the subsurface data, and Y. Lagabrielle, B. Corre, M. Ford, C. Aubourg, N. Espurt, J. Canérot and other colleagues of the PYRAMID and BRGM-RGF programs, as well as S. Calassou, E. Masini and L. Moen-Maurel from TOTAL, for helpful discussions. Comments by P. Agard, editor, and two anonymous reviewers greatly helped to improve the manyscript.

References

Alimen, H., Crouzel, F., Debourle, A., Fourmentraux, J., Henry, J., Delmas, M., Deloffre, R., Debushaye, J., 1963. Carte géol. France (1/50 000), feuille Pau (XV-45), Service de la Carte Géologique de la France, Paris.

Angrand, P., Ford, M., Watts, A.B., 2018. Lateral variations in foreland flexure of a rifted continental margin: The Aquitaine Basin (SW France). Tectonics, 37, 430-449. https://doi.org/10.1002/2017TC004670.

Asti, R., Lagabrielle, Y., Fourcade, S., Corre, B., Monié, P., 2019. How do continents deform during mantle exhumation? Insights from the northern Iberia inverted paleopassive margin, western Pyrenees (France). Tectonics, 38, 1666–1693. https://doi. org/10.1029/2018TC005428.

Barnett-Moore, N., Hosseinpour, M., Maus, S., 2016. Assessing discrepancies between, previous plate kinematic models of Mesozoic Iberia and their constraints. Tectonics, 35, 1843–1862. http://dx.doi.org/10.1002/2015TC004019.

Biteau, J.-J., Le Marrec, A., Le Vot, M., Masset, J.-M., 2006. The Aquitaine Basin. Pet. Geosci., 12, 247-273.

Boirie, J.-M., Souquet, P., 1982. Les poudingues de Mendibelza: dépôts de cônes sous-marins du rift albien des Pyrénées. Bull. Centr. Rech. Explor.-Prod. Elf Aquitaine, 6, 405-435.

Bosch, G., Teixell, A., Jolivet, M., Labaume, P., Stockli, D., Domènech, M., Monié, P., 2016. Timing of Eocene-Miocene thrust activity in the Western Axial Zone and Chaînons Béarnais (west-central Pyrenees) revealed by multi-method thermochronology. Compt. Rendus Geosci., 348, 246-256. http://dx.doi.org/10.1016/j.crte.2016.01.001.

Bourrouilh, R., Richert, J.-P., Zolnaï, G., 1995. The North Pyrenean Aquitaine Basin, France: Evolution and hydrocarbons, A. A. P. G. Bull., 79, 831-853.

Bronner, A., Sauter, D., Manatschal, G., Péron-Pinvidic, G., Munschy, M., 2011. Magmatic breakup as an explanation for magnetic anomalies at magma-poor rifted margins. Nat. Geosci., 4, 549–553. DOI: 10.1038/NGEO1201.

Brun, J.-P., Fort, X., 2004. Compressional salt tectonics (Angolan margin). Tectonophysics, 382, 129-150. doi:10.1016/j.tecto.2003.11.014.

Brun, J.-P., Fort, X., 2011. Salt tectonics at passive margins: Geology versus models. Mar. Pet. Geol., 28, 1123-1145. doi:10.1016/j.marpetgeo.2011.03.004.

Caldera, N., Teixell, A., Griega, A., Labaume, P., Lahfid, A., 2019. Alpine ductile deformation in the Mesozoic cover of the Axial Zone of the Pyrenees (Eaux-Chaudes massif). Geophys. Res. Abstr., 21 (EGU2019-9922, E. G. U. General Assembly, 7-12 April 2019, Vienna).

Canérot, J., 1964. Contribution à l'étude géologique des chaînons nord-pyrénéens compris entre les vallées d'Aspe et d'Ossau (B.P.), Thèse 3e Cycle, Université de Toulouse.

Canérot, J., 1988. Manifestations de l'halocinèse dans les chaînons béarnais (Zone Nord-Pyrénéenne) au Crétacé inférieur. C. R. Acad. Sci. Paris, Série II, 306, 1099-1102.

Canérot, J., 1989. Rifting éocrétacé et halocinèse sur la marge ibérique des Pyrénées occidentales (France). Conséquences structurales. Bull. Centres Rech. Explor.-Prod. Elf-Aquitaine, 13, 87-89.

Canérot, J., 2017. The pull apart-type Tardets-Mauléon Basin, a key to understand the formation of the Pyrenees. BSGF - Earth Sciences Bulletin, 188, 35. DOI: 10.1051/bsgf/2017198.

Canérot, J., Peybernès, B., Ciszak, R., 1978. Présence d'une marge méridionale à l'emplacement de la zone des Chaînons Béarnais (Pyrénées basco-béarnaises). Bull. Soc. géol. France, XX, 673-676.

Canérot, J., Lenoble, J.-L., 1993. Diapirisme crétacé sur la marge ibérique des Pyrénées occidentales : exemple du pic de Lauriolle ; comparaison avec l'Aquitaine, les Pyrénées centrales et orientales. Bull. Soc. géol. France, 164, 719-726.

Canérot, J., Majesté-Menjoulas, C., Ternet, Y., 1999. Le cadre stratigraphique et géodynamique des altérites et des bauxites sur la marge ibérique des Pyrénées occidentales (France). C. R. Acad. Sci. Paris, 328, 451-456.

Canérot, J., Majesté-Menjoulas, C., Ternet, Y., 2001. La faille nord-pyrénéenne, mythe ou réalité ? Strata, 37, 1-31.

Canérot, J., Hudec, M.R., Rockenbauch, K., 2005. Mesozoic diapirism in the Pyrenean orogen: Salt tectonics on a transform plate boundary. A. A. P. G. Bull., 89, 211–229. https://doi.org/10.1306/09170404007.

Casteras, M., Blanc, R., Deloffre, R., Godechot, Y., Labourguigne, J., Villanova, M., Azambre, B., Alimen, M.-H., 1970a. Carte géol. France (1/50 000), feuille Lourdes (1052), BRGM, Orléans.

Casteras, M., Canérot, J., Paris, J.-P., Tisin, D., Azambre, B., Alimen, M.-H., 1970b. Carte géol. France (1/50 000), feuille Oloron-Sainte-Marie (1051), BRGM, Orléans.

Casteras, M., Souquet, P., 1970. Carte géol. France (1/50 000), feuille Larrau (1068), BRGM, Orléans.

Choukroune, P., Mattauer, M., 1978. Tectonique des plaques et Pyrénées : sur le fonctionnement de la faille transformante nord-pyrénéenne ; comparaison avec les modèles actuels. Bull. Soc. géol. France, XX, 689-700.

Clerc, C., Lagabrielle, Y., 2014. Thermal control on the modes of crustal thinning leading to mantle exhumation: Insights from the Cretaceous Pyrenean hot paleomargins. Tectonics, 33, 1340–1359. doi:10.1002/2013TC003471.

Clerc, C., Lahfid, A., Monié, P., Lagabrielle, Y., Chopin, C., Poujol, M., Boulvais, P., Ringenbach, J.-C., Masini, E., de St Blanquat, M., 2015. High-temperature metamorphism during extreme thinning of the continental crust: a reappraisal of the north Pyrenean paleo-passive margin. Solid Earth Discuss., 7, 797-857. doi:10.5194/se-6-643-2015.

Clerc, C., Lagabrielle, Y., Labaume, P., Ringenbach, J.-C., Vauchez, A., Nalpas, T., Bousquet, R., Ballard, J.F., Lahfid, A., Fourcade, S., 2016. Basement – cover decoupling and progressive exhumation of metamorphic sediments at hot rifted margin. Insights from the Northeastern Pyrenean analog. Tectonophysics, 686, 82–97. https://doi.org/10.1016/j.tecto.2016.07.022.

Cloix, A., 2017. Bréchification de la série prérift Nord-Pyrénéenne : Mécanismes tectoniques ou/et sédimentaires et place dans l'histoire tectono-métamorphique de la marge extensive crétacée et de son inversion pyrénéenne (Chaînons Béarnais, Zone Nord-Pyrénéenne). Université de Montpellier, Master Géosciences, Mémoire de Master 2. http://rgf.brgm.fr/sites/default/files/upload/documents/production-scientifique/Masters/rgf_amipyr2016_ma12_memoire_cloix.pdf.

Chochelin, B., Chardon, D., Denèle, Y., Gumiaux, C., Le Bayon, B., 2017. Vertical strain partitioning in hot Variscan crust: Syn-convergence escape of the Pyrenees in the Iberian-Armorican syntax. BSGF - Earth Sci. Bull., 188, 39. https://doi.org/10.1051/bsgf/2017206.

Combes, P.-J., Peybernès, B., Leyreloup, A.-F., 1998. Altérites et bauxites, témoins des marges européenne et ibérique des Pyrénées occidentales au Jurassique supérieur, à l'ouest de la vallée d'Ossau (Pyrénées-Atlantiques, France). C. R. Acad. Sci. Paris, 327, 271-278.

Corre, 2017. La bordure nord de la plaque ibérique à l'Albo-Cénomanien. Architecture d'une marge passive de type ductile (Chaînons Béarnais, Pyrénées Occidentales). Thèse de Doctorat, Université de Rennes 1.

Corre, B., Lagabrielle, Y., Labaume, P., Fourcade, S., Clerc, C., Ballèvre, M., 2016. Deformation associated with mantle exhumation in a distal, hot passive margin environment: New constraints from the Saraillé Massif (Chaînons Béarnais, North-Pyrenean Zone). Comptes Rendus-Geoscience, 348, 279–289. https://doi.org/10.1016/j.crte.2015.11.007.

Curnelle, R., 1983. Evolution structuro-sédimentaire du Trias et de l'infra-Lias d'Aquitaine. Bull. Centres Rech. Explor.-Prod. Elf-Aquitaine, 7, 69-99.

Davis, D.M., Engelder, T., 1985. The role of salt in fold and thrust belts. Tectonophysics, 119, 67-88.

Debroas E.-J., 1987. Modèle de basin triangulaire à l'intersection de décrochements divergents pour le fossé albo-cénomanien de la Ballongue (zone nord-pyrénéenne, France). Bull. Soc. géol. France, III, 887-898.

Debroas, E.-J., 1990. Le Flysch noir albo-cénomanien témoin de la structuration albienne à sénonienne de la Zone nord-pyrénéenne en Bigorre (Hautes-Pyrénées, France). Bull. Soc. géol. France, VI, 273-285.

Debroas, E.-J., Canérot, J., Bilotte, M., 2010. Les Brèches d'Urdach, témoins de l'exhumation du manteau pyrénéen dans un escarpement de faille vraconnien-cénomanien inférieur (zone nord-pyrénéenne, Pyrénées-Atlantiques, France). Géol. France, 2, 53-63.

Dubos-Sallée, N., Nivière, B., Lacan, P., Hervouët., Y., 2007. A structural model for the seismicity of the Arudy (1980) epicentral area (Western Pyrenees, France). Geophys. J. Int., 171, 259–270. doi: 10.1111/j.1365-246X.2007.03499.x.

Ducasse, L., Vélasque, P.-C., Muller, J., 1986. Glissement de couverture et panneaux basculés dans la région des Arbailles (Pyrénées occidentales) : un modèle évolutif crétacé de la marge nord-ibérique à l'Est de la transformante de Pamplona. C. R. Acad. Sc. Paris, Série II, 303, 1477-1482.

Ducoux, M., 2017. Structure, thermicité et évolution géodynamique de la Zone Interne Métamorphique des Pyrénées. Thèse de Doctorat, Université d'Orléans.

Ducoux, M., Jolivet, L., Callot, J.-P., Aubourg, C., Masini, E., Lahfid, A., Homonnay, E., Cagnard, F., Gumiaux, C., Baudin, T., 2019. The Nappe des Marbres unit of the Basque-Cantabrian Basin: the tectono-thermal evolution of a fossil hyperextended rift basin. Tectonics, 38. doi: 10.1029/2018TC005348.

Dumont, T., Replumaz, A., Rouméjon, S., Briais, A., Rigo, A., Bouillin, J.-P., 2015. Microseismicity of the Béarn range: reactivation of inversion and collision structures at the northern edge of the Iberian plate. Tectonics, 34, 934-950. doi: 10.1002/2014TC003816.

Durand-Wackenheim, C., Souquet, P., Thiébaut, G., 1981. La brèche d'Errozaté (Pyrénées-Atlantiques) : faciès de resedimentation en milieu profond de matériaux d'une plateforme carbonatée crétacée à substratum hercynien. Bull. Soc. Hist. nat. Toulouse, 117, 87-94.

Espurt, N., Angrand, P., Teixell, A., Labaume, P., Ford, M., de Saint Blanquat, M., Chevrot, S., 2019. Crustal-scale balanced cross-section and restorations of the Central Pyrenean belt (Nestes-Cinca transect): Highlighting the structural control of Variscan belt and Permian-Mesozoic rift systems on mountain building. Tectonophysics, 764, 25-45. https://doi.org/10.1016/j.tecto.2019.04.026.

Etheve, N., Mohn, G., Frizon de Lamotte, D., Roca, E., Tugend, J., Gómez-Romeu, J., 2018. Extreme Mesozoic Crustal Thinning in the Eastern Iberia Margin: The example of the

Columbrets Basin (Valencia Trough). Tectonics, 37, 636–662. https://doi.org/10.1002/2017TC004613.

Ferrer, O., Jackson, M.P.A., Roca, E., Rubinat, M., 2012. Evolution of salt structures during extension and inversion of the offshore Parentis Basin (Eastern Bay of Biscay). In: Alsop, G.I. et al. (Eds.), Salt Tectonics, Sediments and Prospectivity, Geol. Soc., London, Speci. Publ., 363, 361-379. http://dx.doi.org/10.1144/SP363.16.

Fortané, A., Duée, G., Lagabrielle, Y., Coutelle, A., 1986. Lherzolites and the western «Chaînons béarnais» (French Pyrenees): Structural and paleogeographical pattern. Tectonophysics, 129, 81-98.

García-Senz, J., Pedrera, A., Ayala, C., Ruiz-Constán, A., Robador, A., Rodríguez-Fernández, L.R., 2019. Inversion of the north Iberian hyperextended margin: the role of exhumed mantle indentation during continental collision. In: Hammerstein, J.A., et al. (Eds.), Fold and Thrust Belts: Structural Style, Evolution and Exploration, Geol. Soc., London, Spec. Publ., 490. doi: 10.1144/SP490-2019-112.

Gómez-Romeu, J., Masini, E., Tugend, J., Ducoux, M., Kusznir, N., 2019. Role of rift structural inheritance in orogeny highlighted by the Western Pyrenees case-study. Tectonophysics, 766, 131-150. https://doi.org/10.1016/j.tecto.2019.05.022.

Grool, A.R., Ford, M., Vergés, J., Huismans, R.S., Christophoul, F., Dielforder, A., 2018. Insights into the crustal-scale dynamics of a doubly vergent orogen from a quantitative analysis of its forelands: A case study of the Eastern Pyrenees. Tectonics, 37, 450–476. https://doi.org/10.1002/2017TC004731.

Haller, P., Jardiné, C., 1986. Etude structurale de terrain dans les Chaînons béarnais entre les vallées d'Aspe et d'Ossau. Ecole Nationale Supérieure du Pétrole et des Moteurs-Elf-Aquitaine, Réf. I. F. P. 34115.

Hudec, M.R., Jackson, M.P.A., 2001. The Salt Mine: A Digital Atlas of Salt Tectonics. In: Udden Book Series No 5; A. A. P. G. Memoir, 99. The University of Texas at Austin, Bureau of Economic Geology (305pp).

Jackson., M.P.A., Hudec, M.R., 2017. Salt Tectonics. Cambridge University Press (498pp).

Jackson, C.A.L., Jackson, M.P., Hudec, M.R., 2015. Understanding the kinematics of salt-bearing passive margins: A critical test of competing hypotheses for the origin of the Albian Gap, Santos Basin, offshore Brazil. Geol. Soc. Am. Bull., 127, 1730-1751. doi: 10.1130/B31290.1.

James, V., 1998. La plate-forme carbonatée ouest-pyrénéenne au Jurassique moyen et supérieur : Stratigraphie séquentielle, stades d'évolution, relations avec la subsurface en Aquitaine méridionale. Thèse de Doctorat, Université Paul Sabatier de Toulouse (417pp).

James, V., Canérot, J., 1999. Diapirisme et structuration post-triasique des Pyrénées occidentale et de l'Aquitaine méridionale (France). Eclogae Geol. Helv., 92, 63-72.

James, V., Canérot, J., Biteau, J.-J., 1996. Données nouvelles sur la phase de rifting atlantique des Pyrénées occidentales au Kimméridgien : la masse glissée d'Ouzous (Hautes Pyrénées). Géol. France, 3, 60-66.

Jammes, S., Manatschal, G., Lavier, L., Masini, E., 2009. Tectono-sedimentary evolution related to extreme crustal thinning ahead of a propagating ocean: the example of the western Pyrenees. Tectonics, 28, TC4012. doi:10.1029/2008TC002406.

Jammes, S., Manatschal, G., Lavier, L., 2010. Interaction between prerift salt and detachment faulting in hyperextended rift systems: The example of the Parentis and Mauléon basins (Bay of Biscay and western Pyrenees). A. A. P. G. Bull., 94, 957-975. DOI:10.1306/12090909116.

Johnson, J.A., Hall, C.A.Jr., 1989. Tectono-stratigraphic model for the Massif d'Igountze-Mendibelza, western Pyrenees. J. Geol. Soc. Lond., 146, 925-932.

Jurado, M.J., 1990. El Triásico y el Liásico basal evaporíticos del subsuelo de la cuenca del Ebro. In: Ortí, F., Salvany, J.M. (Eds.), Formaciones Evaporíticas de la Cuenca del Ebro y Cadenas Periféricas, y de la Zona de Levante, ENRESA-Univ. de Barcelona, Barcelona, 54–58.

Kergaravat, C., Ribes, C., Callot, J.-P., Ringenbach, J.-C., 2017. Tectono-stratigraphic evolution of salt-controlled minibasins in a fold and thrust belt, the Oligo-Miocene central Sivas Basin. J. Struct. Geol., 102, 75-97. http://dx.doi.org/10.1016/j.jsg.2017.07.00.

Labaume, P., Meresse, F., Jolivet, M., Teixell, A., Lahfid, A., 2016. Tectonothermal history of an exhumed thrust-sheet-top basin: An example from the south Pyrenean thrust belt. Tectonics, 35, 1280-1313. doi:10.1002/2016TC004192.

Labaume P., Teixell, A., 2018. 3D structure of subsurface thrusts in the eastern Jaca Basin, southern Pyrenees. Geol. Acta, 16, 477-498. DOI: 10.1344/GeologicaActa2018.16.4.9.

Lagabrielle, Y., Bodinier, J.L., 2008. Submarine reworking of exhumed subcontinental mantle rocks: field evidence from the Lherz peridotites, French Pyrenees. Terra Nova, 20, 11-21. doi: 10.1111/j.1365-3121.2007.00781.x.

Lagabrielle, Y., Labaume, P., de Saint Blanquat, M., 2010. Mantle exhumation, crustal denudation, and gravity tectonics during Cretaceous rifting in the Pyrenean realm (SW Europe): Insights from the geological setting of the lherzolite bodies. Tectonics, 29, TC4012. doi:10.1029/2009TC002588.

Lagabrielle, Y., Asti, R., Fourcade, S., Corre, B., Labaume, P., Uzel, J., Clerc, C., Lafay, R., Picazo, S., 2019a. Mantle exhumation at magma-poor passive continental margins. Part II: Tectonic and metasomatic evolution of large-displacement detachment faults preserved in a fossil distal margin domain (Saraillé lherzolites, north-western Pyrenees, France). BSGF-Earth Sci. Bull., 190, 14. https://doi.org/10.1051/bsgf/2019013.

Lagabrielle, Y., Asti, R., Fourcade, S., Corre, B., Poujol, M., Uzel, J., Labaume, P., Clerc, C., Lafay, R., Picazo, S., Maury, R., 2019b. Mantle exhumation at magma-poor passive continental margins. Part I. 3D architecture and metasomatic evolution of a fossil exhumed mantle domain (Urdach lherzolite, north-western Pyrenees, France). BSGF-Earth Sci. Bull., 190, 8. https://doi.org/10.1051/bsgf/2019007.

Lagabrielle, Y., Asti, R., Duretz, T., Clerc, C., Fourcade, S., Teixell, A., Labaume, P., Corre, B., Saspiturry, N., 2020. A review of Cretaceous smooth-slopes-extensional basins along the Iberia-Eurasia plate boundary: how prerift salt controls the modes of continental rifting and mantle exhumation. Earth Sci. Rev., 201. https:/doi.org/10.1016/j.earscirev.2019.103071.

Lanusse, R., 1969. Contribution à l'étude géologique des chaînons calcaires nord-pyrénéens au sud de Saint-Pé-de-Bigorre (H.-P.). Université de Bordeaux, Faculté des Sciences, Mémoire de Diplôme d'Etudes Supérieures.

Lenoble, J.-L., 1992. Les plateformes carbonatées ouest-pyrénéennes du Dogger à l'Albien. Thèse de Doctorat, Université Paul Sabatier de Toulouse.

Lenoble, J.-L., Canérot, J., 1992. La lame extrusive de Pont Suzon (Zone Nord-Pyrénéenne en Vallée d'Aspe) : reprise pyrénéenne d'une ride diapirique transverse d'âge crétacé. C. R. Acad. Sci. Paris, 314, 387-391.

López-Mir, B., Muñoz, J.A., García-Senz, J., 2014. Extensional salt tectonics in the partially inverted Cotiella post-rift basin (south-central Pyrenees): structure and evolution. Int. J. Earth Sci. (Geol Rundsch), 104, 419-434. DOI 10.1007/s00531-014-1091-9.

Masini, E., Manatschal, G.,·Tugend, J.,·Mohn, G., Flament, J.-M., 2014. The tectono-sedimentary evolution of a hyper‐extended rift basin: the example of the Arzacq–Mauléon rift system (Western Pyrenees, SW France). Int. J. Earth Sci. (Geol Rundsch). DOI 10.1007/s00531-014-1023-8.

Mediavilla, F., Mauriaud, P., 1987. La tectonique salifère d’Aquitaine. Pétrole et Techniques, 335, 35-41.

Menant, A., Aubourg, C., Cuyala, J.-B., Hoareau, G., Callot, J.-P., Péré , E., Labaume, P., Ducoux, M., 2016. Salt tectonics and thermal imprint along an inverted passive margin: the Montcaou anticline, Chaînons Béarnais, North Pyrenean Zone. Geophysical Research Abstracts, 18, EGU2016-15281, E. G. U. General Assembly, 17-22 April 2016, Vienna.

Montigny, R., Azambre, B., Rossy, M., Thuizat, R., 1986. K-Ar study of Cretaceous magmatism and metamorphism in the Pyrenees: Age and length of rotation of the Iberian peninsula. Tectonophysics, 129, 257–273. doi:10.1016/0040-1951(86)90255-6.

Mouthereau, F., Filleaudeau, P.-Y., Vacherat, A., Pik, R., Lacombe, O., Fellin, M.G., Castelltort, S., Christophoul, F., Masini, E., 2014. Placing limits to shortening evolution in the Pyrenees: Role of margin architecture and implications for the Iberia/Europe convergence. Tectonics, 33, 2283-2314. doi:10.1002/2014TC003663.

Muñoz, J.A., Beamud, E., Fernández, O., Arbués, P., Dinarès-Turell, J., Poblet, J., 2013. The Ainsa fold and thrust oblique zone of the central Pyrenees: Kinematics of a curved contractional system from paleomagnetic and structural data. Tectonics, 32, 1142-1175. doi:10.1002/tect.20070, 2013.

Nirrengarten, N., Manatschal, G., Tugend, J., Kusznir, N., Sauter, D., 2018. Kinematic evolution of the southern North Atlantic: implications for the formation of hyper-extended rift systems. Tectonics, 37, 89-118. https://doi.org/ 10.1002/2017TC004495.

Ortí, F., Pérez-López, A., Salvany, J.M. 2017. Triassic evaporites of Iberia: Sedimentological and palaeogeographical implications for the western Neotethys evolution during the Middle Triassic–Earliest Jurassic. Palaeogeogr., Palaeoclimatol., Palaeoecol., 471, 157–180. doi: 10.1016/j.palaeo.2017.01.025.

Paris, J.-P., 1969. Observations géologiques dans la région du pic de Layens (Basses-Pyrénées). Bull. Soc. Hist. Nat. Toulouse, 105, 270-278.

Pedrera, A., García-Senz, J., Ayala, C., Ruiz-Constán, A., Rodríguez-Fernández, L.R., Robador, A., González Menéndez, L., 2017.Reconstruction of the exhumed mantle across the North Iberian Margin by crustal-scale 3-D gravity inversion and geological cross section. Tectonics, 36, 3155-3177. https://doi.org/10.1002/2017TC004716.

Pichel, L.M., Jackson, C.A.L., Pell, F., Dooley, T.P., 2019. Base-salt relief controls on salt-tectonic structural style, São Paulo Plateau, Santos Basin, Brasil. Basin Res., 00, 1-32. doi: 10.1111/bre.12375.

Puigdefábregas, C., Souquet, P., 1986. Tecto-sedimentary cycles and depositional sequences of the Mesozoic and Tertiary from the Pyrenees. Tectonophysics, 129, 173-203.

Roux, J.-C., 1983. Recherches stratigraphiques et sédimentologiques sur les flyschs crétacés pyrénéens au sud d'Oloron (Pyrénées-Atlantiques). Thèse de 3ème Cycle, Université Paul-Sabatier, Toulouse,.

Rowan, M.G.F., Lawton, T.F., Vendeville, B.C., 2004. Gravity-driven fold belts on passive margins. In: McClay, K.R. (Ed.), Thrust Tectonics and Hydrocarbon Hystems, A. A. P. G. Mem,. 82, 157-182.

Santolaria, P., Casas-Sainz, A.M., Soto, R., Pinto, V., Casas, A., 2014. The Naval diapir (southern Pyrenees): Geometry of a salt wall associated with thrusting at an oblique ramp. Tectonophysics, 637, 30–44. https://doi.org/10.1016/j.tecto.2014.09.008.

Saspiturry, N., Razin, P., Baudin, T., Serrano, O., Issautier, B., Lasseur, E., Allanic, C., Thinon, I., Leleu, S., 2019. Symmetry vs. asymmetry of a hyper-thinned rift: Example of the Mauléon Basin (Western Pyrenees, France). Mar. Petr. Geol., 104, 86-105. https://doi.org/10.1016/j.marpetgeo.2019.03.031.

Saura, E., Ardèvol, I., Oro, L., Teixell, A., Vergés, J., 2016. Rising and falling diapirs, shifting depocenters, and flap overturning in the Cretaceous Sopeira and Sant Gervàs subbasins (Ribagorça Basin, southern Pyrenees). Tectonics, 35, 638-662. doi:10.1002/2015TC004001.

Séguret, M., 1972. Etude tectonique des nappes et séries décollées de la partie centrale du versant sud des Pyrénées. Caractère synsédimentaire, rôle de la compression et de la gravité. Montpellier, Publications de l'Université des Sciences et Techniques du Languedoc, série Géologie Structurale, 2.

Serrano, O., 2001. Le Crétacé supérieur-Paléogène du bassin compressif Nord-Pyrénéen (Bassin de l'Adour). Sédimentologie, Stratigraphie, Géodynamique. Thèse de Doctorat, Université de Rennes 1, Mémoires Géosciences Rennes, 101.

Serrano, O., Delmas, J., Hanot, F., Vially, R., Herbin, J.-P., Houel, P., Tourlière, B., 2006. Le Bassin d'Aquitaine : valorisation des données sismiques, cartographie structurale et potentiel pétrolier, Ed. BRGM, Orléans.

Soto, J.I., Flinch, J.F., Tari, G., 2017. Permo-Triassic Basins and Tectonics in Europe, North Africa and the Atlantic Margins: A Synthesis. In: Soto, J.I., Flinch, J.F., Tari, G. (Eds.), Permo-

Triassic Salt Provinces of Europe, North Africa and the Atlantic Margins, Tectonics and Hydrocarbon Potential, Elsevier, Amsterdam, pp. 3-41..

Souquet, P., Debroas, E.-J., Boirie, J.-M., Pons, P., Fixari, G., Roux, J.-C., Dol, J., Thieuloy, J.-P., Bonnemaison, M., Manivit, H., Peybernès, B., 1985. Le groupe du flysch noir (Albo-Cénomanien) dans les Pyrénées. Bull. Centres Rech. Explor-Prod. Elf-Aquitaine, 9, 183–252.

Teixell, A., 1990. Alpine thrusts at the western termination of the Pyrenean Axial Zone. Bull. Soc. géol. France, 8, 241-249.

Teixell, A., 1993. Coupe géologique du massif d'Igountze : implications sur l'évolution structurale de la bordure sud de la Zone nord-pyrénéenne occidentale. C. R. Acad. Sci. Paris, 316, 1789-1796.

Teixell, A., 1996. The Ansó transect of the southern Pyrenees: basement and cover thrust geometries. J. Geol. Soc. Lond., 153, 301-310.

Teixell, A., Labaume, P., Lagabrielle, Y., 2016. The crustal evolution of the west-central Pyrenees revisited: Inferences from a new kinematic scenario. Compt. Rendus Geosci., 348, 257-267. https://doi.org/10.1016/j.crte.2015.10.010.

Teixell, A., Labaume, P., Ayarza, P., Espurt, N., de Saint Blanquat, M., Lagabrielle, Y., 2018. Crustal structure and evolution of the Pyrenean-Cantabrian belt: A review and new interpretations from recent concepts and data. Tectonophysics, 724, 146-170. doi:10.1016/j.tecto.2018.01.009.

Ternet, Y., Barrère, P., Bois, J.-P., Soulé, J.-C., 1980. Carte géol. France (1/50 000), feuille Argelès-Gazost (1070), BRGM, Orléans.

Ternet, Y., Barrère, P., Canérot, J., Majesté-Menjoulàs, C., 2004. Carte géol. France (1/50 000), feuille Laruns-Somport (1069), BRGM, Orléans.

Tugend, J., Manatschal, G., Kusznir, N.J., Masini, E., Mohn, G., Thinon, I., 2014. Formation and deformation of hyperextended rift systems: Insights from rift domain mapping in the Bay of Biscay-Pyrenees. Tectonics, 33, 1239-1276. doi:10.1002/2014TC003529.

Vacherat, A., Mouthereau, F., Pik, R., Bernet, M., Gautheron, C., Masini, E., Le Pourhiet, L., Tibaric, B., Lahfid., A., 2014. Thermal imprint of rift-related processes in orogens as recorded in the Pyrenees. Earth Planet. Sci. Letters, 408, 296-306. http://dx.doi.org/10.1016/j.epsl.2014.10.014.

Vacherat, A., Mouthereau, F., Pik, R., Bellahsen, N., Gautheron, C., Bernet, M., Daudet, M., Balansa, J., Tibari, B., Pinna Jamme, R., Radal, J., 2016. Rift-to-collision transition recorded by tectonothermal evolution of the northern Pyrenees. Tectonics, 35, 907-933. doi: 10.1002/2015TC004016.

Villard, J., 2016. Déformation et thermicité de la couverture mésozoïque dans une structure salifère des Chaînons Béarnais (Zone Nord Pyrénéenne), Université de Montpellier, Master Géosciences, Mémoire de Master 2. http://rgf.brgm.fr/sites/default/files/upload/documents/production-scientifique/Masters/rgf_amipyr2015_ma7_memoire_villard.pdf.

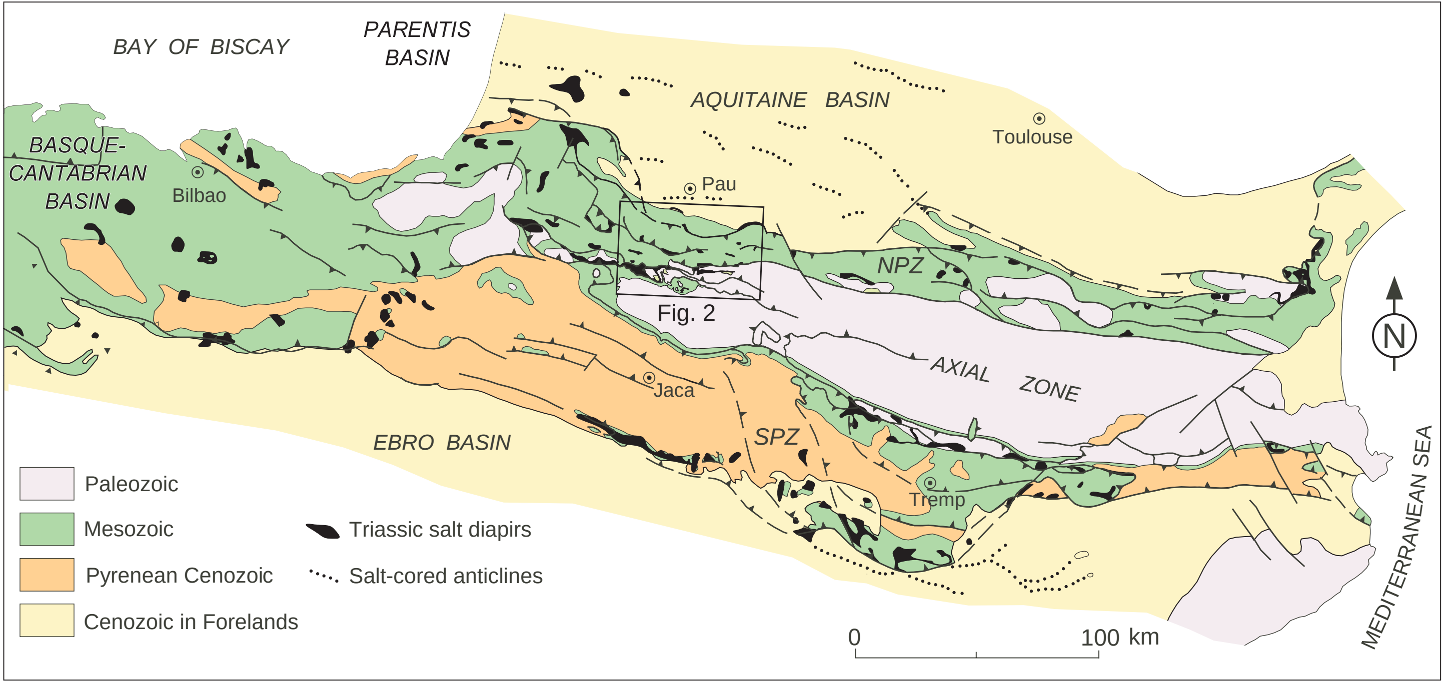

Fig. 1. Structural sketch map of the Pyrenees with location of the main outcrops of Triassic Keuper evaporitic facies. Map modified from Teixell (1996) and Saura et al. (2016). NPZ: North Pyrenean Zone; SPZ: South Pyrenean Zone.

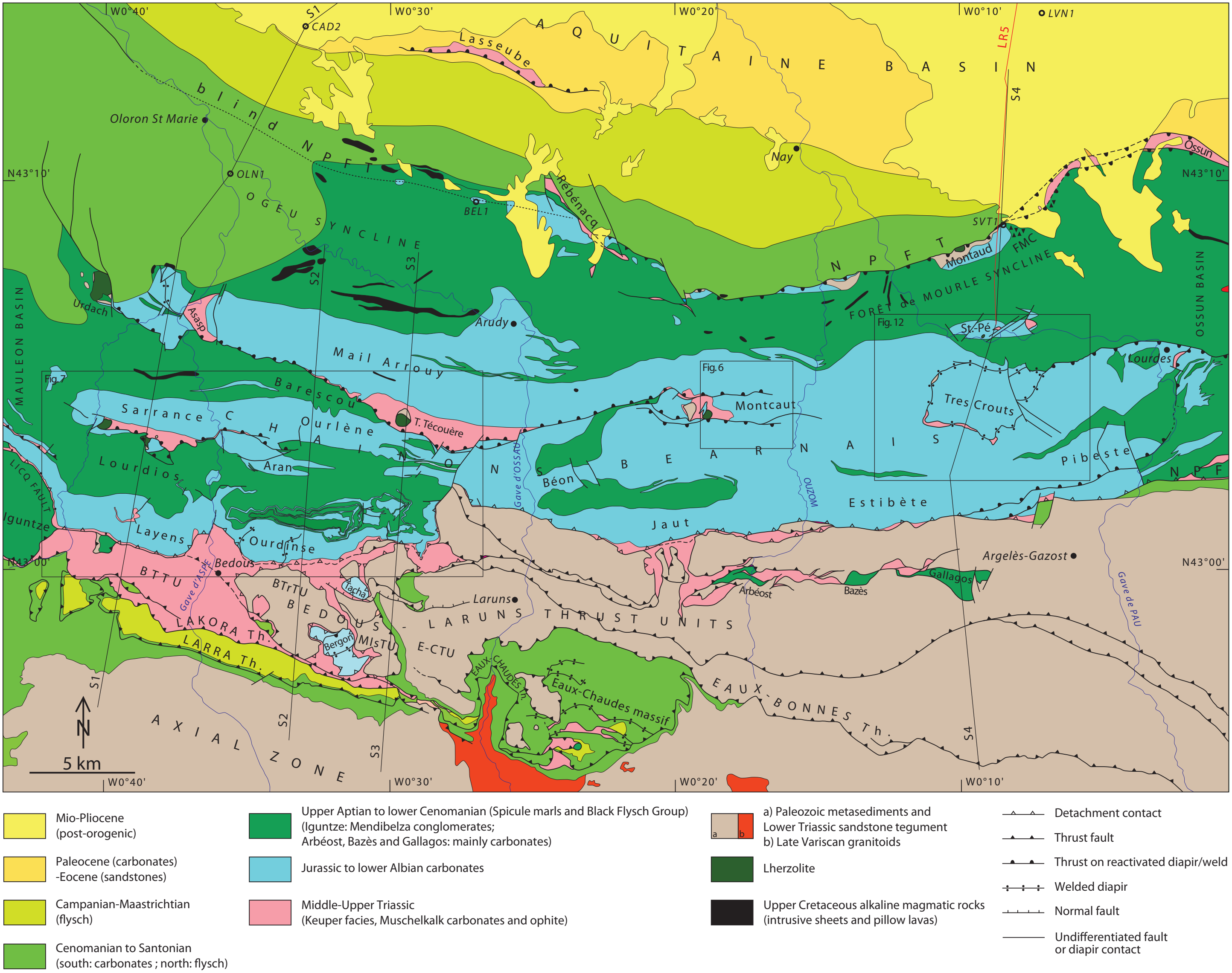

Fig. 2. Geological map of the Chaînons Béarnais belt (North-Pyrenean Zone) and adjacent areas. The so-called "Chaînons Béarnais" are the anticline and thrust ridges of Jurassic to lower Albian carbonates (in blue). BTrTU: Bois de la Traillère thrust unit; BTTU: Bedous Triassic thrust unit; E-CTU: Eaux-Chaudes fold-thrust unit; FMC: Forêt de Mourle Albian conglomerates; MIsTU: Montagnon d'Iseye thrust unit; NPF: North-Pyrenean Fault; NPFT: North-Pyrenean Frontal Thrust. S1 to S4: cross-sections in Fig. 4 (S1 extends 1.8 km north of the map boundary, in the area of post-orogenic sediment exposure). LR5: seismic profile in Supplementary Data, Fig. S2. Wells: BEL1, Bélair 1; CAD2: Cardesse 2; LVN1: Livron 1; OLN1, Oloron 1; SVT1: Saint Vincent 1 (see well stratigraphic logs in Supplementary Data, Fig. S1). Map sources: BRGM 1:50,000 scale geological maps (Alimen et al., 1963; Casteras et al., 1970a and b; Ternet et al., 1980, 2004), Souquet et al. (1985) and original mapping (in frames of Figs. 7 and 12).

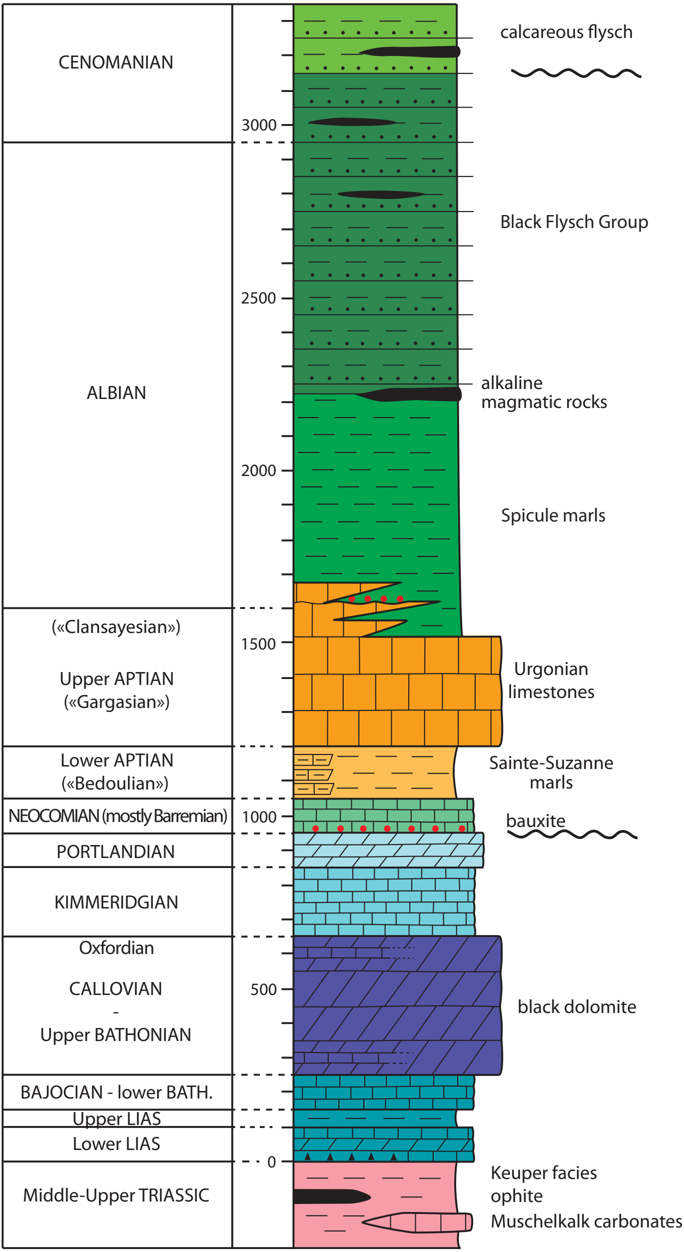

Fig. 3. Simplified stratigraphic log of the Chaînons Béarnais belt. Local unconformities are shown. Red dots: alterite horizons (including bauxite). Based on Casteras et al. (1970a and b), Souquet et al. (1985), Lenoble (1992), James (1998).

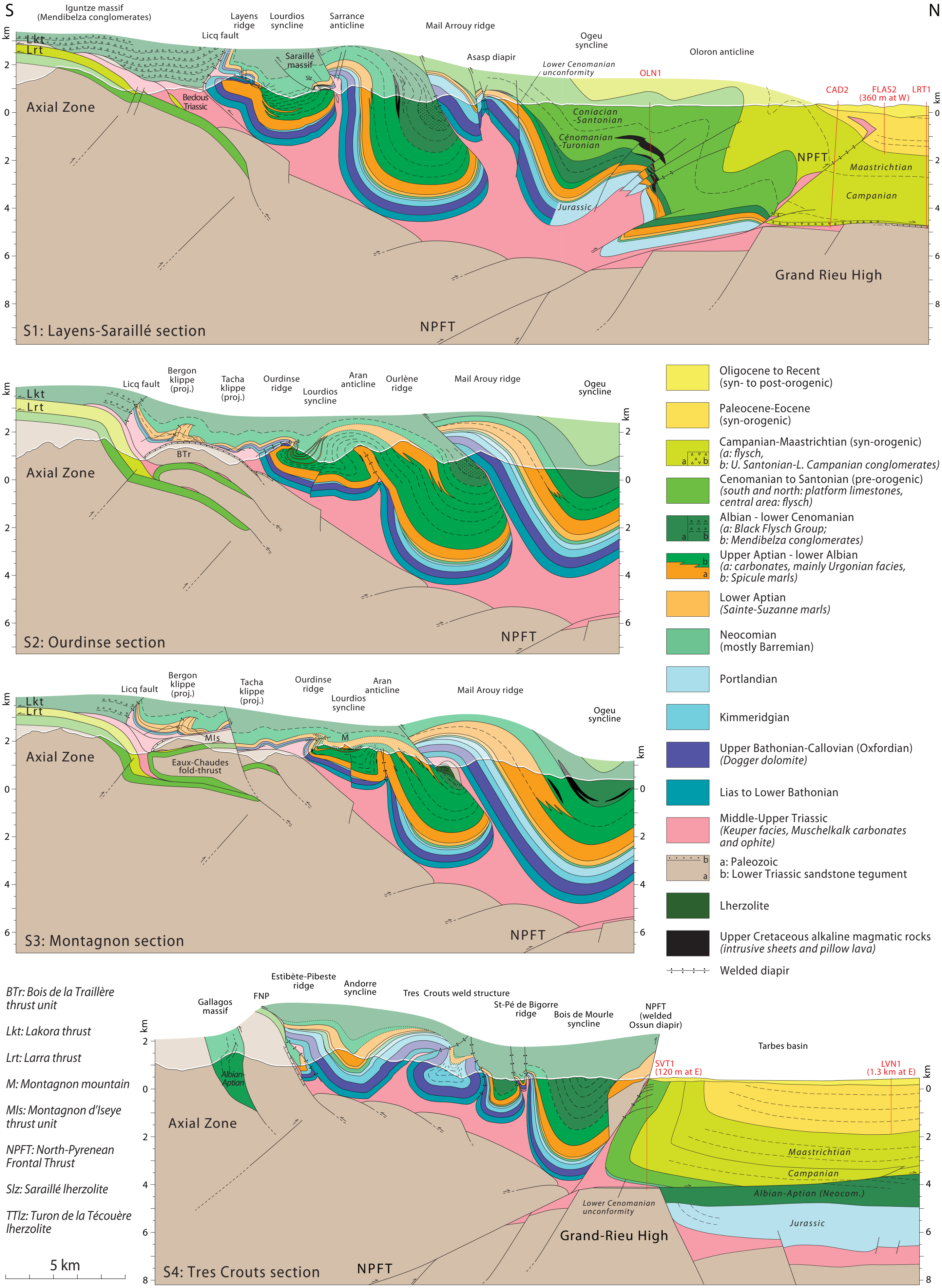

Fig. 4. Geological sections across the Chaînons Béarnais belt. See location in Fig. 2. FNP: North Pyrenean fault. Wells: CAD2: Cardesse 2; FLAS2: Lasseube 2; LRT1: Le Rouat 1; LVN1: Livron 1; OLN1: Oloron 1; SVT1; Saint Vincent 1 (see well stratigraphic logs in Supplementary Data, Fig. S1). Northern part of S4 cross-section includes interpretation of the regional seismic profile n°5 from Serrano et al. (2006) (see location in Fig. 2, and the interpreted profile in Supplementary Data, Fig. S2).

Fig. 5. Field images of the Chaînons Béarnais stratigraphic units. (a): Panorama of the Mail Arrouy carbonate ridge featuring the Middle-Upper Triassic complex and the Jurassic-Lower Cretaceous carbonate succession in the hanging wall of the Mail Arrouy thrust (cf. stratigraphic log in Fig. 3 and cross-section S3 in Fig. 4). The Triassic contains the Turon de la Técouère lherzolite and adjacent lens of Paleozoic metasediments. The unit is thrust southwards over the upper Aptian limestones of the Ourlène carbonate ridge (foreground). The Aquitaine Basin is in the background (with the Pau city in the middle part). Photograph taken from 703300E, 4769070N (UTM coordinates, zone 30T). (b): Syn-metamorphic bedding-parallel foliation in the upper Aptian Urgonian facies limestones, featuring flattened bivalves (rudists; eastern Ourdinse ridge; 705380E, 4765900N). (c): Syn-metamorphic bedding-parallel foliation in the Albian flysch (Lourdios syncline; 689240E, 4768790N).

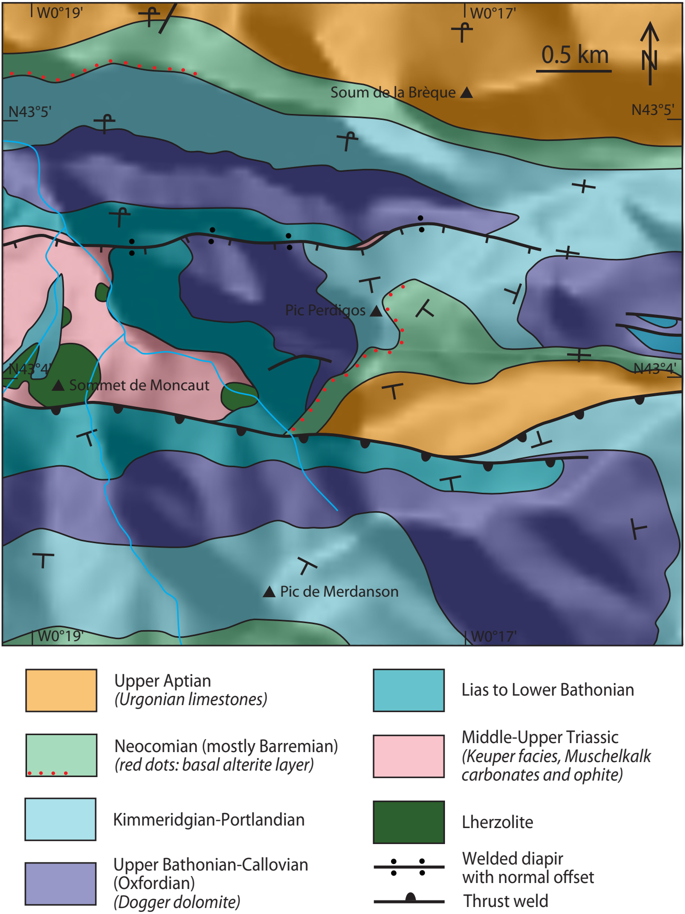

Fig. 6. Geological map of the Moncaut salt anticline showing the Lower Cretaceous unconformity on top of a former diapir crest (near Pic Perdigos). See location in Fig. 2. Map simplified from Casteras et al. (1970a).

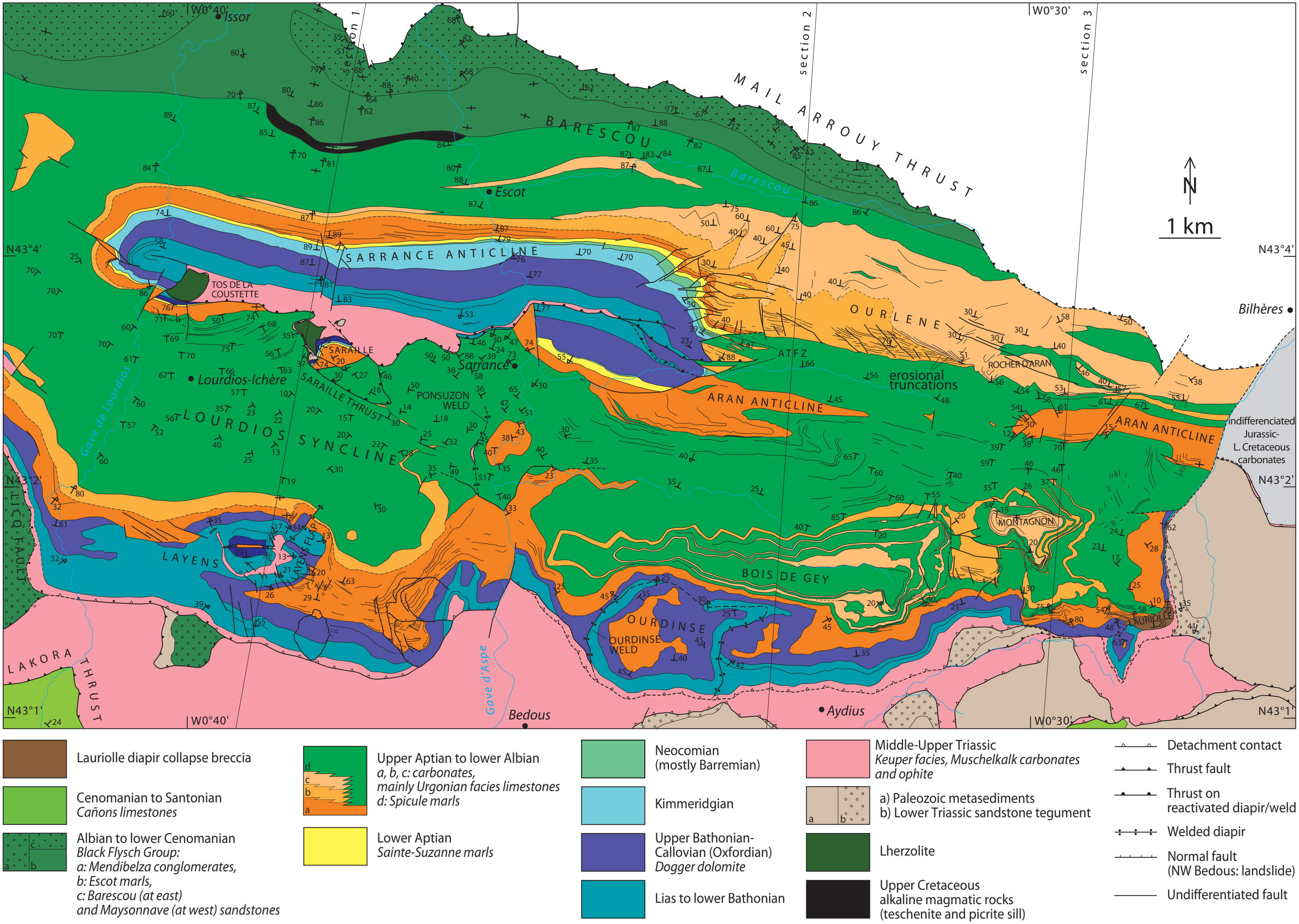

Fig. 7. Geological map of the Lourdios and Barescou minibasins and adjacent carbonate ridges (SW Chaînons Béarnais). See location in Fig. 2 and cross-sections S1 to S3 in Fig. 4. Map sources: mainly original mapping on the field and aerial photographs, with complements from Canérot (1964), Paris (1969) and Casteras et al. (1970b). The Urgonian limestones are divided into three stratigraphic members. The lower interval corresponds mostly to the Gargasian and the two upper intervals to the Clansayesian, possibly reaching the lower Albian. However, the limits given to these members may not strictly correspond to time-lines across the whole map. ATFZ: Aran transverse fault zone.

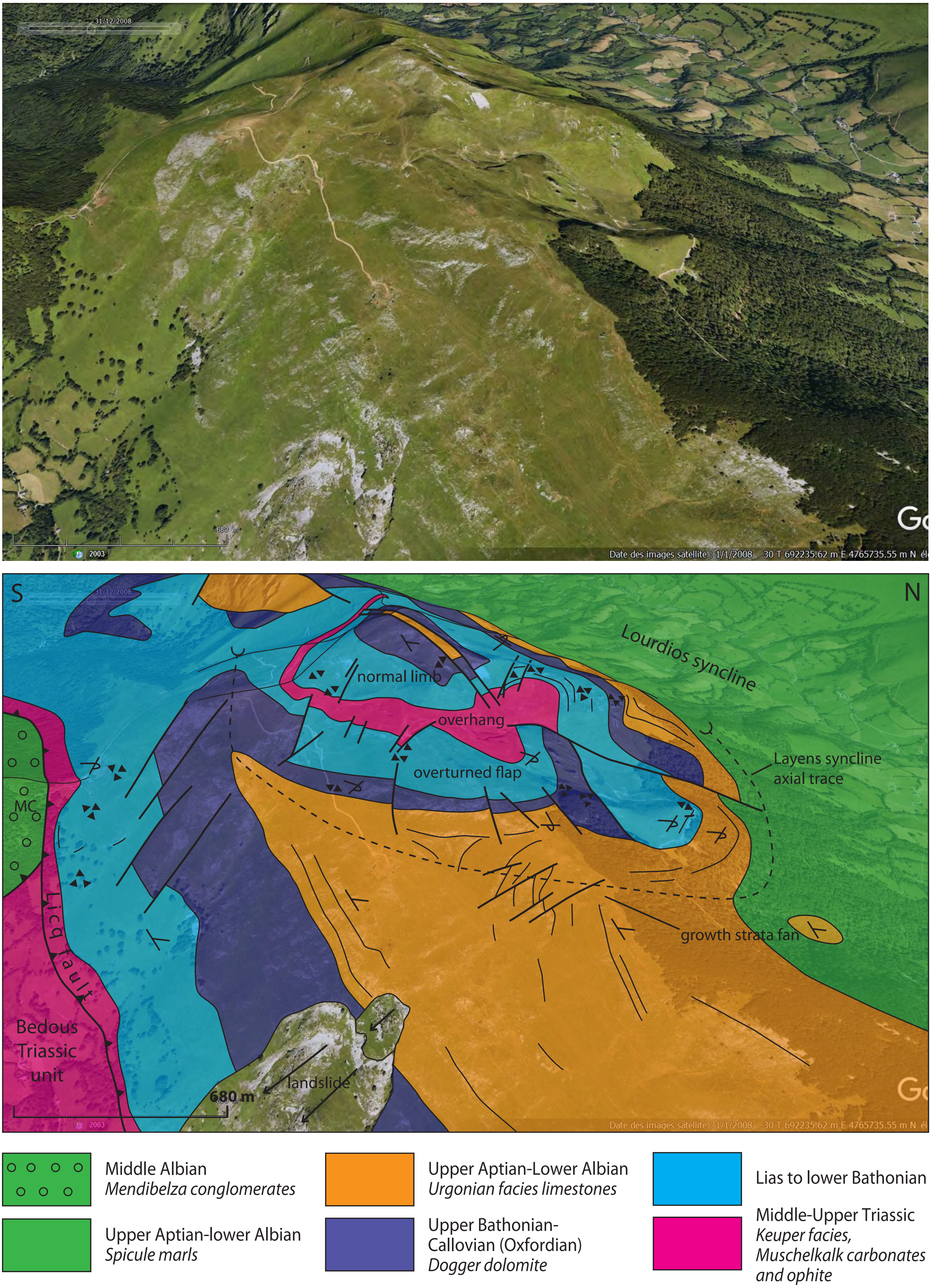

Fig. 8. Layens overhang at the southern edge of the Lourdios minibasin (Layens carbonate ridge). Google Earth oblique view from the SE. For lithostratigraphy see the stratigraphic log in Fig. 3. See location of the Layens carbonate ridge in Fig. 7, and cross-section of the diapiric structure in S1 in Fig. 4. The figure illustrates the curved axial trace of the recumbent syncline and strong thickness reduction of the Dogger dolomite and Urgonian limestones in the overturned flap and above-lying normal limb, due to the Neocomian erosion of the Dogger and to growth folding in the Urgonian, evidencing diapir rise during the Early Cretaceous. Diapir rising, collapse and erosion induced frequent brecciation in the Lias and Dogger (triangles), and steeply-dipping faults, probably related to diapir collapse, may correspond to welded diapir piercings.

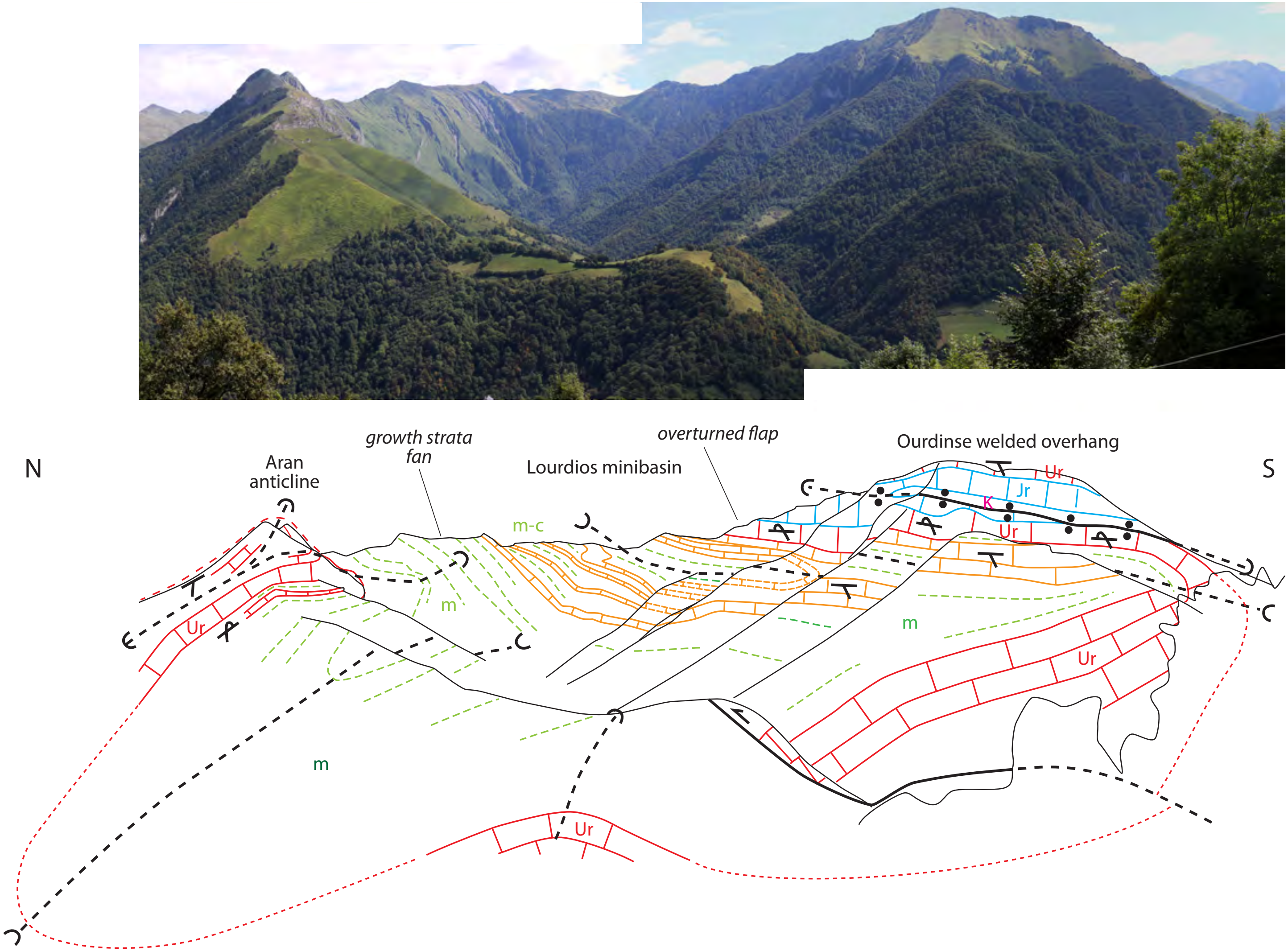

Fig. 9. Lourdios minibasin, Bois de Gey panorama. Key: Jr: Jurassic, K: Triassic Keuper facies, m-c: uppermost Aptian (Clansayesian) (to lower Albian?) marls with limestone intercalations, Ur: upper Aptian limestones (Urgonian facies), cf. stratigraphic log in Fig. 3. See location of the Aran and Ourdinse carbonate ridges in Fig. 7, and cross-section of the structure in S2 in Fig. 4. View from 694042E, 4768258N. The figure illustrates the pouch-like geometry of the syncline minibasin with both limbs featuring overturned flaps and growth strata fans. The reverse fault at bottom right may correspond to a tilted and deformed syn-sedimentary normal fault.

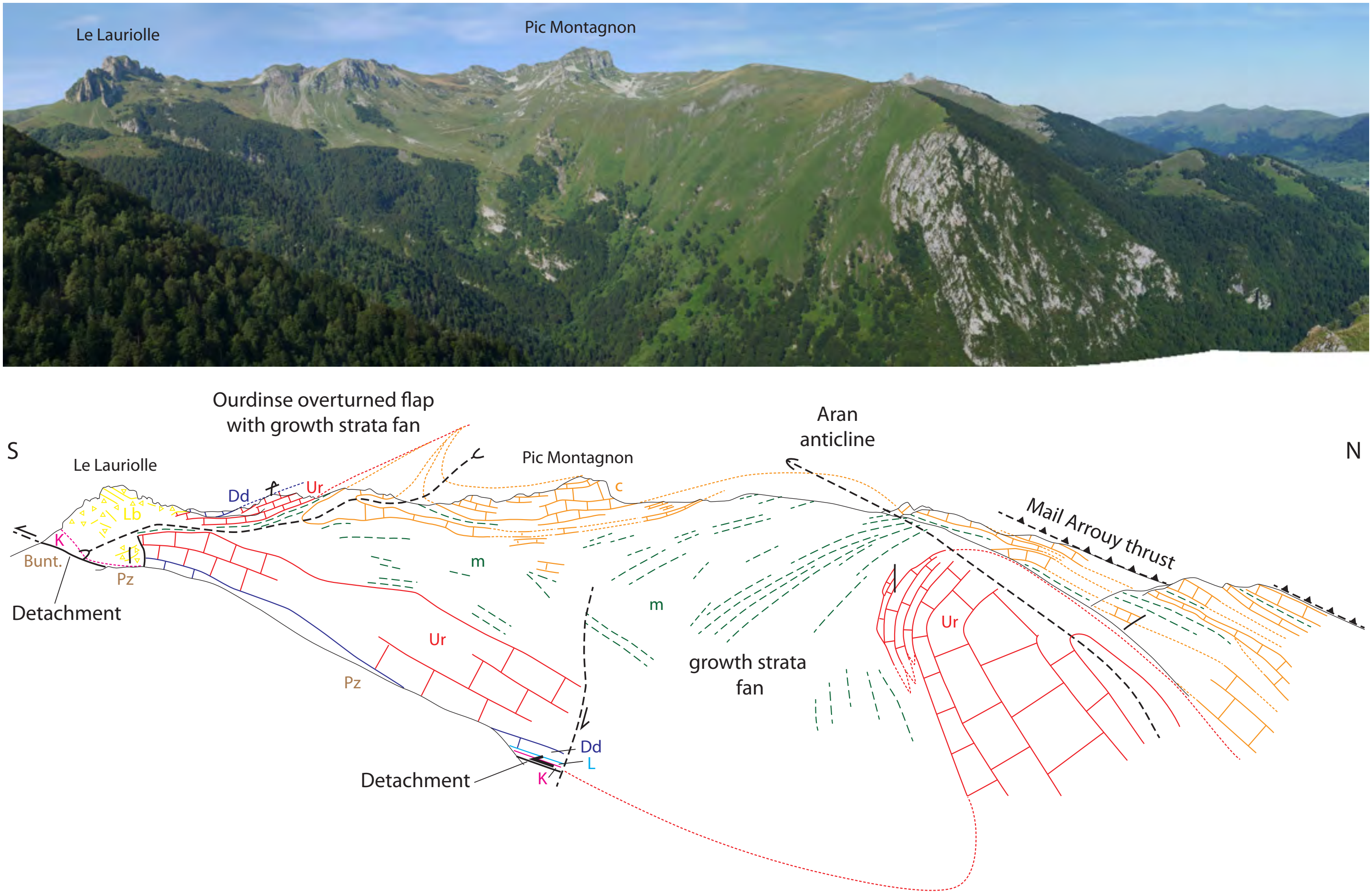

Fig. 10. Lourdios minibasin, Pic Montagnon panorama. Key: Bunt: Lower Triassic sandstone tegument (Buntsandstein facies), c: uppermost Aptian (Clansayesian) (to lower Albian?) carbonates (limestones with local dolomitization) intercalations in the marls (m), Dd: Dogger dolomite, L: Liassic limestones, Lb: Lauriolle breccia, K: Triassic Keuper facies, Pz: Paleozoic metasediments, Ur: upper Aptian limestones (Urgonian facies). See location of Le Lauriolle, Pic Montagnon and Aran anticline in Fig. 7, and cross-section of the structure in S3 in Fig. 4. View from 707538E, 4767470N. The figure illustrates the pouch-like geometry of the syncline minibasin with both limbs featuring overturned flaps and growth strata fans. The reverse fault at bottom may correspond to a tilted and deformed syn-sedimentary normal fault. At left, the Lauriolle breccia results from diapir collapse (Canérot and Lenoble, 1993; Cloix, 2017). The label “detachement” shows the contact of the Mesozoic cover above the Paleozoic and its Buntsandstein tegument, now a sub-vertical contact due to deformation along a transverse Pyrenean structure (the “Ossau thrust” of Canérot, 2017), possibly inherited from the Mesozoic extensional system.

Fig. 11. View of the northward progradation of the upper Aptian limestones at the southern edge of the Barescou minibasin (Rocher d'Aran, Ourlène carbonate ridge). S0/S1: bedding-parallel cleavage, S2: local late cleavage. See location of Rocher d'Aran and Ourlène carbonate ridge in Fig. 7, and cross-section of the structure in S3 in Fig. 4. View from 702533E, 4769493N. The figure illustrates the shelf edge progradation away from the rising crest of the Aran anticline located to the south. The contact between the limestones and underlying marls is affected by dolomitisation (dol.), similarly to most of the marl-limestone contacts on the northern limb of the Aran anticline (Canérot, 1964).

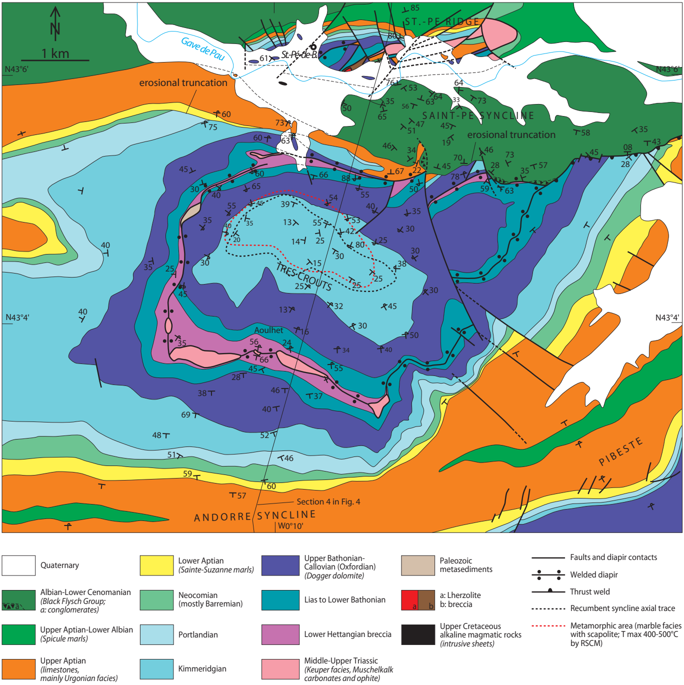

Fig. 12. Geological map of the Tres Crouts polygonal weld structure (location in Fig. 2). See cross-section of the structure in S4 in Fig. 4. Map sources: BRGM 1:50,000 scale geological map (Casteras et al., 1970a), Lanusse (1969), Cloix (2017) and original mapping. The central metamorphic area is marked by marble after the Kimmeridgian limestone, with scapolite crystallization and maximum temperatures recorded up to close to 500°C (Villard, 2016; Ducoux, 2017).

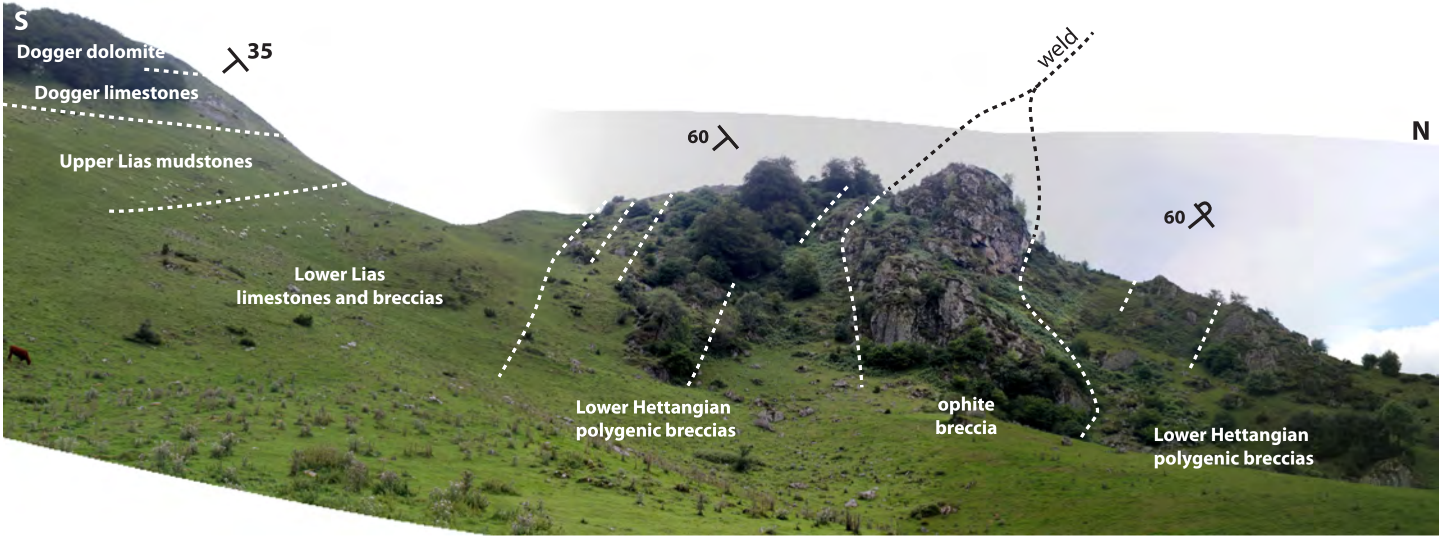

Fig. 13. Panorama of the Tres Crouts weld (southern segment at Aoulhet). See location of Aoulhet in Fig. 12 and cross-section of the structure in S4 in Fig. 4. View from 730728E, 4771609N. A hundred-meter scale block of brecciated Triassic ophite is pinched along the welded base of the Jurassic succession.

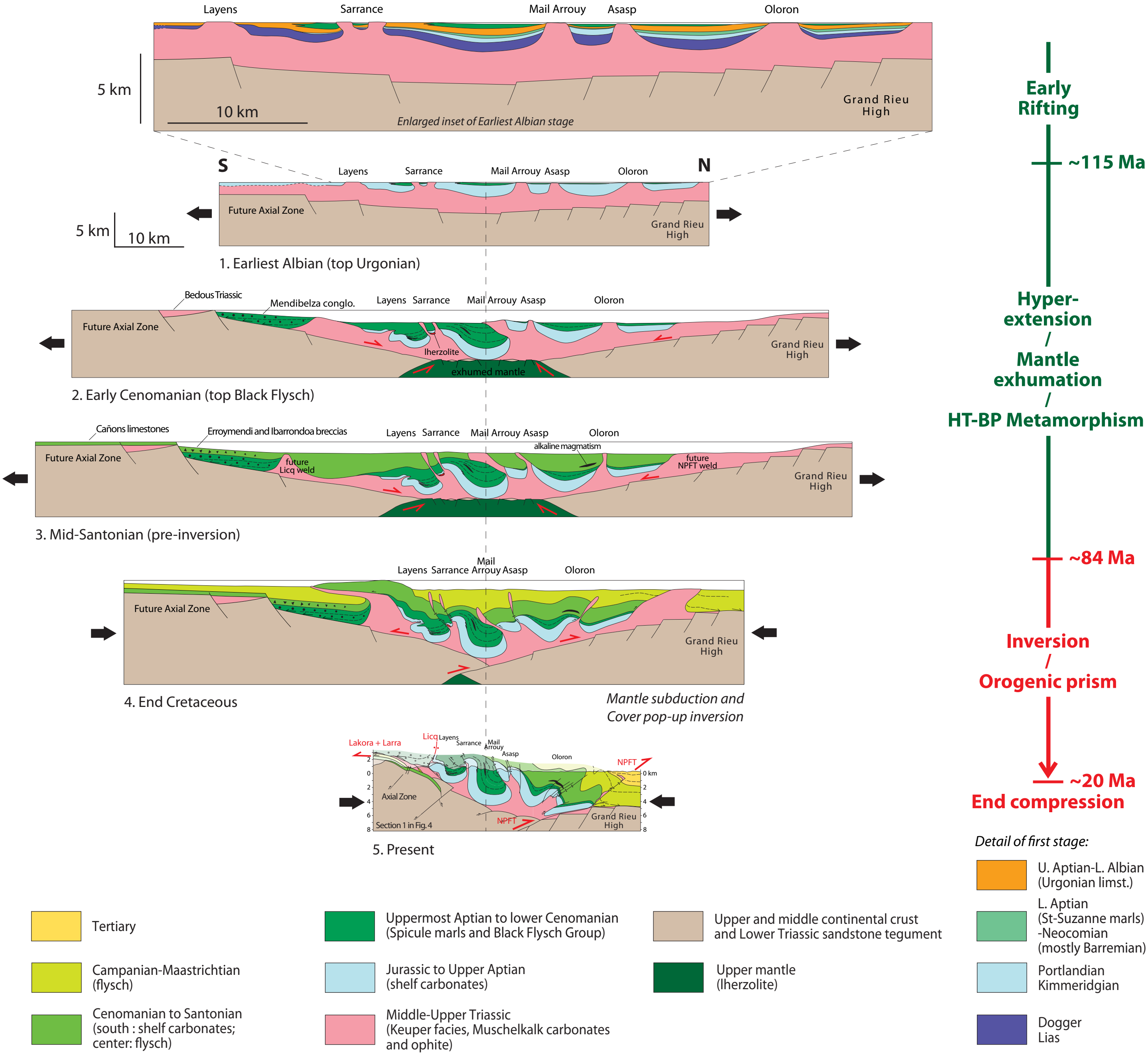

Fig. 14. Kinematic evolution of the North-Pyrenean detached basin and diapiric system during the mid-Cretaceous rifting and the Pyrenean inversion. The structure of the basement top is derived from the model of hyper-extension of Teixell et al. (2016). The present-day stage in 5 corresponds to the Aspe valley cross-section of the Chaînons Béarnais belt (S1 in Fig. 4). See text Section 5 for description.

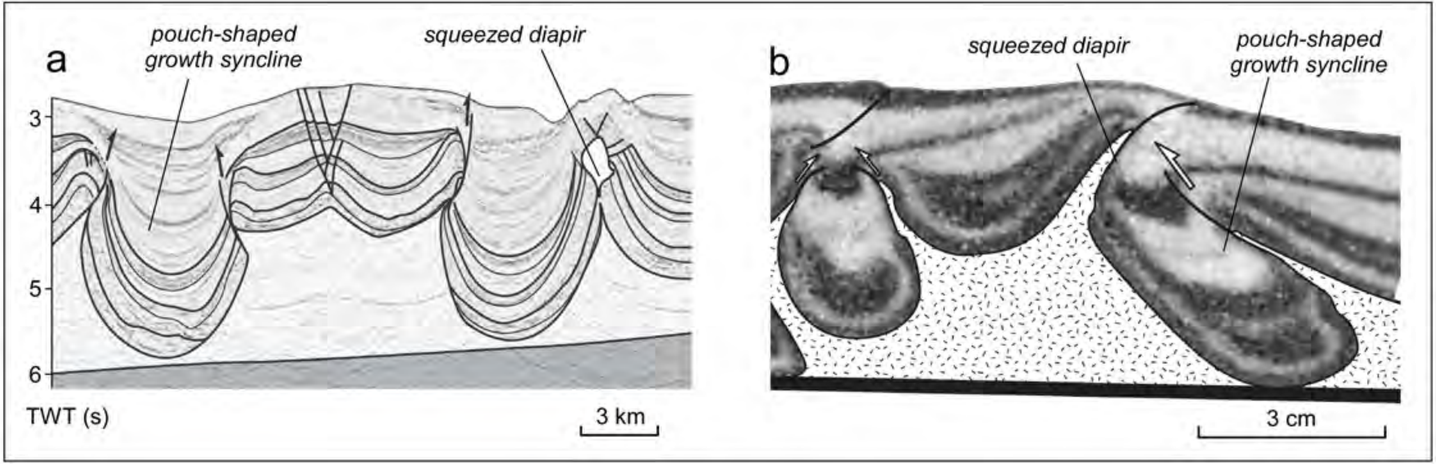

Fig. 15. Examples of (a) a seismic image of the gravity-driven contractional deformation in the Angolan margin and (b) a sandbox model of a contractional salt system (after Brun and Fort, 2004). Note the squeezed diapirs and the intervening, pouch-shaped growth synclines with irregular amplitude and wavelenght that constitute good analogues for the Chaînons Béarnais salt structures shown in Figs. 4 and 14.

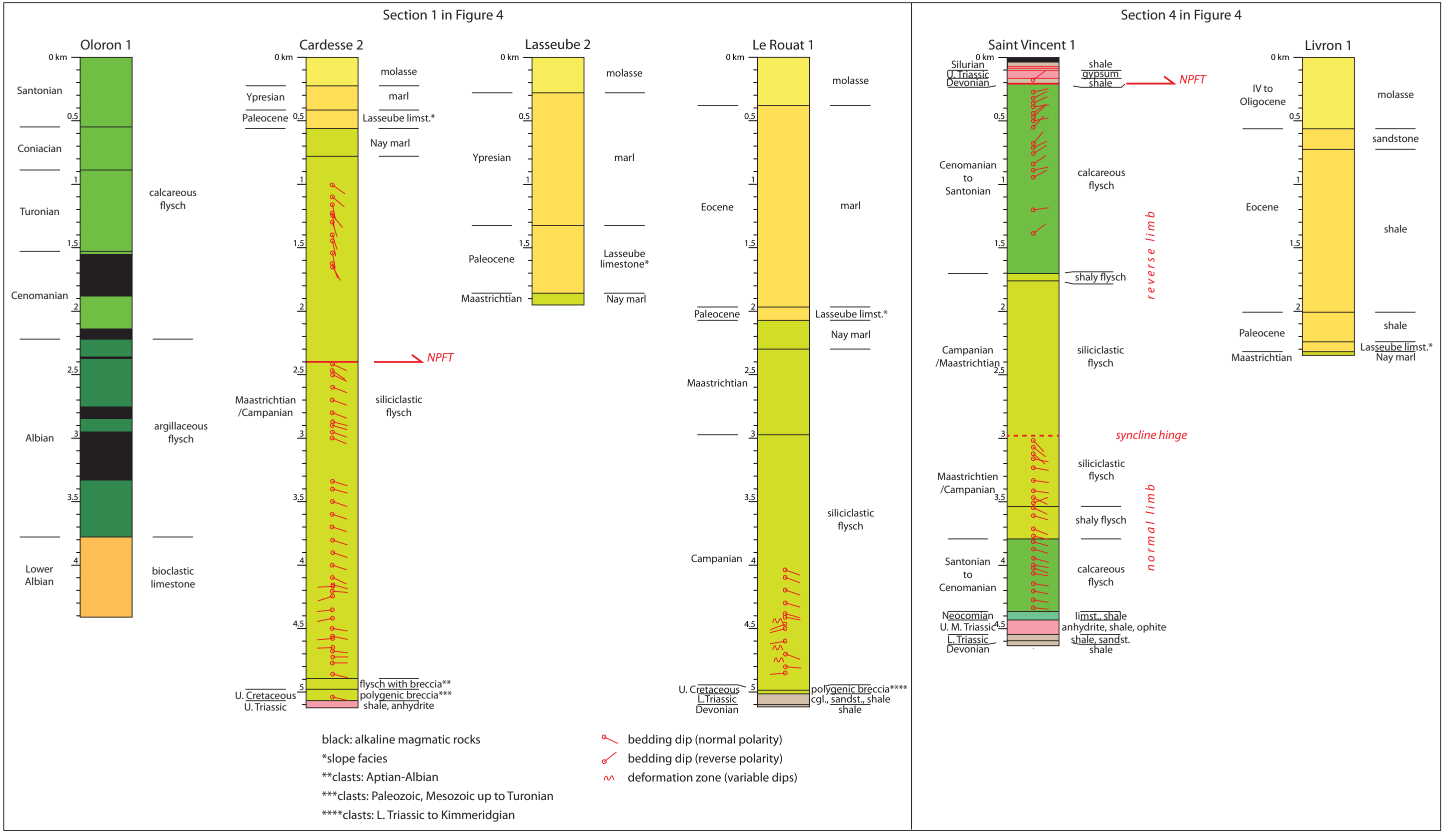

Fig. S1. Stratigraphic logs of wells used in cross-sections S1 and S4 in Figure 4. Original data are in <infoterre.brgm.fr>. NPFT: North Pyrenean Frontal Thrust.

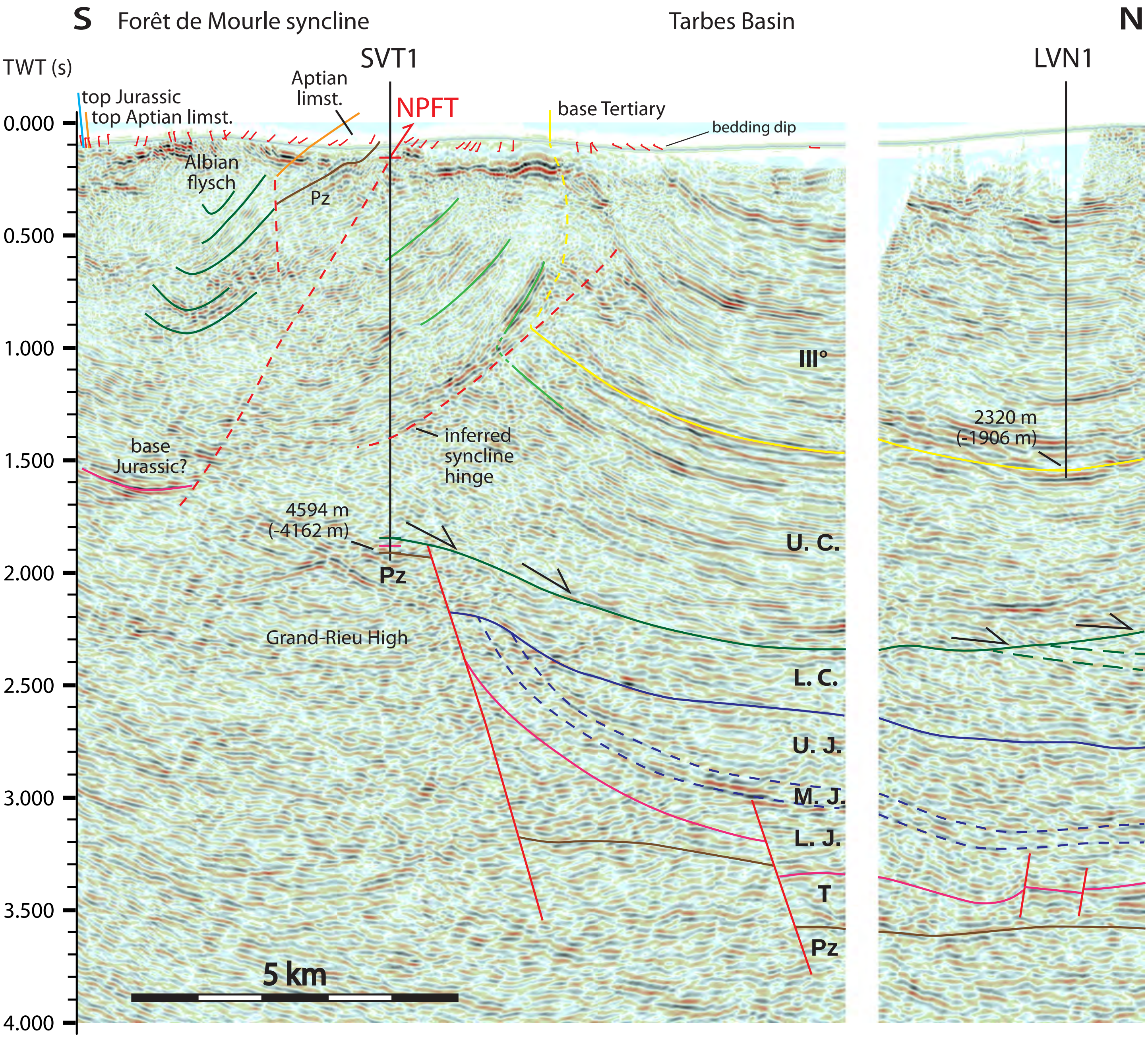

Fig. S2. Seismic reflection profile across the North Pyrenean Frontal Thrust (NPFT) in the northern part of cross-section S4 (Figure 4). It corresponds to the southern part of the Regional Line 5 processed and first published by Serrano et al. (2006). In the present work, the profile was provided by BRGM in the frame of the PYRAMID Project, and it is here visualized with the Kingdom Suite software. Depth-time conversion of wells and geological interpretation north of the Grand-Rieu High are from Serrano et al. (2006), except for the base of the Upper Cretaceous in the northernmost part where we interpret a southward dipping erosional contact in the Albian flysch and onlap of the Upper Cretaceous flysch. Geological interpretation above and south of the Grand-Rieu High and surface bedding dips are from this work. Dips were measured along the trace of the seismic line south of the NPFT and, due to the presence of post-orogenic molasse at the surface, projected from the west in the north. The depths of the basement top in well SVT1 and of the base of Tertiary in well LVN1 are reported (depths measured from the surface and, between parentheses, below sea level) (see Fig. S1). These depths show that seismic velocities are much higher in the NPFT area (well SVT1), probably due to older strata and stronger deformation, than in the younger and little deformed sediments in the Tarbes basin (well LVN1). This results in distortion of the seismic image in the transition zone, preventing good imaging of the structure of the NPFT footwall. Serrano et al. (2006) interpreted a fault between the reverse and normal limbs in the Upper Cretaceous flysch drilled in SVT1 (see bedding dips on well log in Fig. S1) However, the interpretation of an unfaulted syncline with growth strata in the Campanian to Eocene fits better with actual depths in wells, as shown in cross-section S4 in Figure 4. The latter also shows that the top of Lower Cretaceous dips gently southward. NPFT: North-Pyrenean Frontal Thrust; III°: Tertiary; L. C.: Lower Cretaceous; L. J.: Lower Jurassic; M. J.: Middle Jurassic; Pz: Paleozoic; T: Triassic; U. C.: Upper Cretaceous; U. J.: Upper Jurassic. Wells: LVN1: Livron 1; SVT1: Saint-Vincent 1. See well logs in Fig. S1 (including bedding dips for SVT1), and original well data in <infoterre.brgm.fr>.